MS No.: hess-2016-226 by Andreasen et al.
7 March, 2017

Editor

Dear authors,

thanks a lot for the detailed response and the modification in the paper. I think the paper looks now very good and is in general ready for publication in HESS. When studying the revised version, I found some technical corrections and changes that should be included into the final manuscript:

Dear Markus Weiler,

Thank you for your comments. We very much appreciate you taking the time to make these additional edits. Following your suggestions we believe that the readability of the tables and figures has been improved.

Best regards,

Mie Andreasen

Table 5 - please remove the left column with the content "Gludsted Plantation models (Fig. 3)". This is not relevant for the table.

AC1 (Author comment # 1): The left column in Table 5 has been removed. Furthermore, a title (“Models”) has been added to the header row of the (new) left column.

Table 6 - please move the unit of the soil moisture the the header row of the table and also provide a header description for the two left columns

AC2: The unit of soil moisture has not been moved to the header row because other units are provided further down in the column (e.g., centimeters, millimeters and tons per hectare). Instead, an overall title (“Models”) has been included in the header for the two left columns. This is done in order to emphasize that these two columns in total are describing the different models used in the sensitivity analysis. Other small adjustments have been done in order to improve the readability of the table. This includes the naming of the models and the overall setup of the table.

In general, most figures could be simplified by removing the symbols for all modelled data. Usually, observations, as they are not continuous, are illustrated as symbols and simulations are illustrated as lines. This would also help your figures as they are very busy with all the symbols for the simulated neutron intensities (fig 2-5, 8, 9).

AC3: Figures 3-5 and 7-9 have been changed according to the suggested guideline.

Please change the extend of the y axis in Figure 7 - all information is situated between 0.8 and 0.85 - so why showing such a wide range? The legend could me move in between the individual graphs.

AC4: The extent of the y-axis of Figure 7 has been decreased to 0.75 to 0.90. The range is a little wider than the suggested range. This is because the range of t/e ratio values goes a little below 0.80.

Best regards

Markus Weiler

Cosmic-ray neutron transport at a forest field site: the sensitivity to various environmental conditions with focus on biomass and canopy interception

Mie Andreasen[1], Karsten H. Jensen[1], Darin Desilets [2], Marek Zreda [3], Heye R. Bogena[4] and Majken C. Looms[1]

[1] Department of Geosciences and Natural Resource Management, University of Copenhagen, Denmark

[2] Hydroinnova LLC, Albuquerque, New Mexico

[3] Department of Hydrology and Water Resources, University of Arizona, Arizona

[4] Agrosphere IBG-3, Forschungszentrum Juelich GmbH, Germany

Correspondence to: Mie Andreasen (mie.andreasen@ign.ku.dk)

Keywords

1. Cosmic-ray neutron intensity method
2. Neutron transport modeling
3. Canopy interception
4. Forest biomass

Abstract

Cosmic-ray neutron intensity is inversely correlated to all hydrogen present in the upper decimeters of the subsurface and the first few hectometers of the atmosphere above the ground surface. This correlation forms the base of the cosmic-ray neutron soil moisture estimation method. The method is, however, complicated by the fact that several hydrogen pools other than soil moisture affect the neutron intensity. In order to improve the cosmic-ray neutron soil moisture estimation method and explore the potential for additional applications knowledge about the environmental effect on cosmic-ray neutron intensity is essential (e.g., the effect of vegetation, litter layer and soil type). In this study the environmental effect is examined by performing a sensitivity analysis using neutron transport modeling. We use a neutron transport model with various representations of the forest and different parameters describing the subsurface to match measured height profiles and time series of thermal and epithermal neutron intensities at a field site in Denmark. Overall, modeled thermal and epithermal neutron intensities are in satisfactory agreement with measurements, yet, the choice of forest canopy conceptualization is found to be significant. Modeling results show that the effect of canopy interception, soil chemistry and dry bulk density of litter and mineral soil on neutron intensity is small. On the other hand, the neutron intensity decreases significantly with added litter layer thickness, especially for epithermal neutron energies. Forest biomass also has a significant influence on the neutron intensity height profiles at the examined field site, altering both the shape of the profiles and the ground level thermal-to-epithermal neutron ratio. This ratio increases with increasing amounts of biomass, and was confirmed by measurement from three sites representing agricultural, heathland, and forest land cover. A much smaller effect of canopy interception on the ground level thermal-to-epithermal neutron ratio was modeled. Overall, the results suggest a potential to use ground level thermal-to-epithermal neutron ratios to discriminate the effect of different hydrogen contributions on the neutron signal.

1. Introduction

Soil moisture plays an important role in water and energy exchanges at the ground-atmosphere interface, but is difficult to measure at the intermediate spatial scale (hectometers). The cosmic-ray method has been developed to circumvent the shortcomings of existing measurement procedures for soil moisture detection at this scale (e.g. Zreda et al. (2008) and Franz et al. (2012)). The cosmic-ray neutron intensity (eV range) at the ground surface is a product of the elemental composition and density of the surrounding air and soil matrix. Hydrogen is an essential element controlling neutron transport because of its physical properties and often relatively high concentration close to the land surface. As a result, neutron intensity is inversely correlated with the hydrogen content of the surrounding hectometers of air and top decimeters of the ground

(Zreda et al., 2008). Since soil moisture often forms the major dynamic pool of hydrogen within the footprint of the detector, neutron intensity measurements have been found to be suitable for soil moisture estimation.

Nonetheless, cosmic-ray neutron intensity detection also holds a potential for estimating the remaining pools of hydrogen (Zreda et al., 2008; Desilets et al., 2010). Hydrogen is stored statically in water in soil minerals and buildings/roads, quasi-statically in above and below-ground-biomass, soil organic matter, snow and lakes/streams, or dynamically in soil water, atmospheric water vapor and canopy intercepted precipitation (see Table 1).

Table 1 is inserted here

To date, studies have primarily aimed to advance the cosmic-ray neutron method for soil moisture estimation by determining correction models to remove the effect of other influencing pools of hydrogen.

Rosolem et al. (2013) examined the effect of atmospheric water vapor on the neutron intensity (with energies 10-100 eV; 1 eV = $1.6*10^{-19}$ J) using neutron transport modeling and presented a method to rescale the measured neutron intensity to reference conditions. This correction for changes in atmospheric water vapor has become a standard procedure for the preparation of cosmic-ray neutron data along with corrections for temporal variations in barometric pressure and incoming cosmic radiation (Zreda et al., 2012).

Several studies have focused on improving the N_0 calibration parameter used for soil moisture estimation at forest field sites but also at high-yielding crop field sites like maize. Bogena et al. (2013) demonstrated the importance of including the litter layer in the calibration for cosmic-ray neutron soil moisture estimation at field locations with a significant litter layer. Furthermore, the N_0 calibration parameter obtained from field measurements was found to decrease with increasing biomass (Rivera Villarreyes et al., 2011; Hornbuckle et al., 2012; Hawdon et al., 2014; Baatz et al., 2015). In order to account for this effect Baatz et al. (2015a) defined a N_0-based correction model to remove the effect of biomass on the neutron intensity signal. A similar correcting approach to improve the cosmic-ray neutron soil moisture estimation method by removing the influence of biomass and snow was presented by Tian et al. (2016). However, the study distinguishes itself by considering the ratio of the neutron intensity measured by the bare detector and the moderated detector instead of the effect on the N_0 parameter. Iwema et al. (2015) and Heidbüchel et al. (2016) applied the N_0 calibration function and obtained improved cosmic-ray neutron soil moisture estimates by performing more than one calibration campaign per field site and defining a site-specific calibration function. Heidbüchel et al. (2016) speculate that the curve shape of the standard N_0 calibration function is insufficient at the studied forest field site because of the presence of a litter layer and spatially heterogeneous soil moisture conditions within the neutron detector footprint. A different approach was presented by Franz et al. (2013b). Here a universal calibration function was proposed where separate estimates of the various hydrogen pools were included for cosmic-ray neutron soil moisture estimation.

Few studies have explored the potential of using the cosmic-ray neutron method for applications other than soil moisture. Desilets et al. (2010) distinguished snow and rain events using measurements of two neutron energy bands, and Sigouin and

Si (2016) reported an inverse relationship between snow water equivalent and the neutron intensity measured using the moderated detector. Franz et al. (2013a) demonstrated an approach to isolate the effect of vegetation on the neutron intensity signal and estimated area average biomass water equivalent in agreement with independent measurements. The signals of biomass and canopy interception on neutron intensity, measured using the moderated detector, have been investigated by Baroni and Oswald (2015). They accounted the higher soil moisture estimated using the cosmic-ray neutron method compared to the up-scaled soil moisture measured at point-scale to be the impact of canopy interception and biomass. The two pools of hydrogen were then separated in accordance to their dynamics.

The ability to separate the signals of the different hydrogen pools on the neutron intensity is valuable both for the advancement of the cosmic-ray neutron soil moisture estimation method and for the potential of additional applications. The potential of determining canopy interception and biomass from the cosmic-ray neutron intensity is of interest as they represent essential hydrological and ecological variables. Both are difficult and expensive to measure continuously at larger scales.

Canopy interception is for some climatic and environmental settings an important variable to include in water balance studies, as well as in hydrological and climatological modeling. For the forest site studied here the canopy interception loss was found to be 31-34% of the gross precipitation (Ringgaard et al., 2014). A common method to estimate canopy interception is by subtracting the precipitation measured at ground level below canopy (throughfall) from precipitation measured above the forest canopy (gross precipitation) using standard precipitation gauges. However, the spatial scale of measurement is small and is not representative of larger areas as the canopy interception is highly heterogeneous. In order to obtain a representative measure of canopy interception multiple throughfall stations must be installed. This is labor intensive and measurement uncertainties are significant. Precipitation underestimation due to wind turbulence, wetting loss, and forest debris plugging the measurement gauge at the forest floor are sources of uncertainty (Dunkerley, 2000).

The forest biomass represents an important resource for timber industry and renewable energy. Furthermore, forest modifies the weather through the mechanisms and feedbacks related to evapotranspiration, surface albedo and roughness. Carbon sequestration by afforestation and an effective forest management is a widely used method to decrease the concentration of carbon dioxide in the atmosphere and thereby attenuate the greenhouse effect (Lal, 2008). The carbon sequestration in vegetation can be quantified by monitoring the growth of biomass over time. The most conventional and accurate method to estimate forest biomass is the use of allometric models describing the relationship between the biomass of a specific tree species and easily measurable tree parameters, such as tree height and tree diameter at breast height (Jenkins et al., 2003). However, this approach is time consuming and labor intensive because numerous trees have to be surveyed to obtain accurate and representative results (Popescu, 2007). Remote sensing technology offers alternative methods to estimate biomass as high correlations are found between spectral bands and vegetation parameters. One method providing high resolution maps is airborne *Light Detection And Ranging* (LiDAR) technology (Boudreau et al., 2008). The LiDAR system is installed in small aircrafts and digitizes the first and last return of near-infrared laser recordings. The canopy height can be

obtained at decimeter grid-size scale and the biomass can be estimated from regression models. Instruments and aircraft-surveys are expensive, and measurements of tree growth will often be at a coarse temporal resolution.

This study is an initial step towards reaching the overall objective of improving the cosmic-ray neutron soil moisture estimation method, especially at field locations with several pools of hydrogen. Furthermore, we wish to investigate the potential of biomass and canopy interception estimation using the cosmic-ray neutron intensity measurements. Here, the aim is to address this goal using only cosmic-ray neutron intensity measurements and not auxiliary information (e.g., biomass measurements using allometric models and tree surveys).

Previous studies examining the effect of hydrogen on cosmic-ray neutron intensity has for most cases considered a single neutron energy range (neutron intensity measured using the moderated neutron detector) at a single height level (typically 1.5 m above the ground). Thermal and epithermal neutrons are both sensitive to hydrogen. However, they are characterized by very different physical properties and reaction patterns resulting in different height profiles, as well as unique responses to environmental settings at the immediate ground-atmosphere interface. For this reason, thermal and epithermal neutron intensity at multiple height levels above the ground surface are considered in this study as the combination may provide additional information. Furthermore, neutron transport modeling sets the basis for this study. Neutron transport modeling of specific sites is limited and has only been performed for non-vegetated field sites (Franz et al., 2013b; Andreasen et al., 2016). In this context, forest sites are especially complex to conceptualize as the number of free parameters is relatively high (e.g. biomass, litter, soil chemistry, interception and the structure of the forest). Here, we first focus on modeling a forest field site. The model is developed from measured soil and vegetation parameters at the specific locality. The modeled neutron intensity profiles are evaluated against profile measurements, and time-series of neutron intensity measurements at two heights. Following, the environmental impact on thermal and epithermal neutron intensities are identified and quantified by applying a sensitivity analysis. The environmental impact refers to the effect of the specific properties and settings of the field site on neutron transport. This includes vegetation, litter, soil composition and layers, and canopy interception. For the sensitivity analysis, one component at the time is changed in the model and the sensitivity of the component is quantified by calculating the change in the neutron intensity relative to a reference model. Measurements at an agricultural field site with no biomass and at a heather field site with a smaller amount of biomass are used to underpin the influence of certain environmental variables (e.g., biomass, litter layer).

To our knowledge this is the first study based on both measurements and modeling which provides a quantitative analysis of the potential of using the cosmic ray technique for estimation of interception and biomass.

2. Method

2.1. Terminology and neutron energies

The energy of a neutron determines the probability of the neutron interacting with other elements and the type of interaction (i.e. absorbing or scattering). Overall, an important threshold for the behavior of low energy neutrons is present at energies

somewhere below 0.5 eV. The specific energy ranges of thermal, epithermal and fast neutrons are ambiguous. For the purpose of this paper the following terminology for neutron energies is used:

- Thermal: Energy range 0 – 0.5 eV
- Epithermal: Energies above 0.5 eV
- Fast: Energy range 10 - 1000 eV

When modeling neutron transport for hydrological applications it is common to consider fast energy ranges (10 – 100 eV or 10 – 1000 eV) (Desilets et al., 2010; 2013; Rosolem et al., 2013; Franz et al., 2013b; Köhli et al., 2015), while measurements using standard soil moisture neutron detectors are sensitive to the entire epithermal energy range (Andreasen et al., 2016). Here, the term epithermal neutrons will be used for both measured neutrons of energies above 0.5 eV and modeled neutrons of energies 10 – 1000 eV.

The probability of absorption reactions is greater for thermal neutrons, while the probability of scattering reactions is greater for neutrons of epithermal energies. For this reason thermal and epithermal neutron height profiles are very different at the ground-atmosphere interface. The epithermal neutron intensity increases with height above the ground surface as the neutrons at higher elevations have been scattered less than neutrons closer to the ground surface. The production rate of thermal neutrons is high in the soil and low in the air. This is related to the high density of the soil and the low density of air. The absorption rate of thermal neutrons is significant in both the ground and in the air. In the air, this is due to the presences of nitrogen. This results in a decreasing thermal neutron intensity with height until approximately 150 m at which point the thermal neutron intensity is unaffected by the soil. Above this point the thermal neutron intensity will increase with height following a similar curve as neutrons of higher energies.

2.2. Cosmic-ray neutron detection

2.2.1. Equipment

Cosmic-ray neutron intensity was measured using the CR1000/B system from Hydroinnova LLC, Albuquerque, New Mexico. The system has two detectors that consist of tubes filled with boron-10 (enriched to 96%) trifluoride ($^{10}BF_3$) proportional gas. The neutron detection relies on the $^{10}B(n,\alpha)^7Li$ reaction for converting thermal neutrons into charged particles (α) and then into an electronic signal. One detector is unshielded (bare detector), while the other is shielded by 25 mm of high-density polyethylene (moderated detector). These different configurations give the bare and moderated tubes different energy sensitivities.

The thermal neutron absorption cross-section of ^{10}B is very high (3835 barns) (Sears et al., 1992). This absorption cross-section decreases rapidly with increasing neutron energy following a $1/E_n^{0.5}$ law (where E_n is neutron energy) (Knoll 2010). Therefore, the energies measured by the bare tube comprise a continuous distribution which is heavily weighted toward thermal neutrons (<0.5 eV), with a small proportion of epithermal neutrons also being detected (<10%) (Andreasen et al., 2016).

The moderated detector is more sensitive to higher neutron energies (> 0.5 eV). The purpose of the polyethylene is to slow (moderate) epithermal neutrons through interactions with hydrogen in order to increase the probability of them being captured by ^{10}B in the detector. At the same time the polyethylene attenuates the thermal neutron flux through neutron capture by hydrogen. Nonetheless, still a large proportion originates from below 0.5 eV (approximately 40% of the thermal neutrons detected by the bare detector) (Andreasen et al., 2016).

Obeying Poissonian statistics (Knoll 2010) the relative measurement uncertainty of a given neutron intensity, N, decreases with increasing neutron intensity as the standard deviation equals $N^{0.5}$.

The measured neutron intensities are corrected for variations in barometric pressure, atmospheric water vapor and incoming cosmic-ray intensity following procedures of Zreda et al. (2012) and Rosolem et al. (2013). Unfortunately, the water vapor correction of Rosolem et al. (2013) is only valid for epithermal neutron measurements. Since the development of correction methods is beyond the scope of this study, we refrained from using a vapor correction for the measured thermal neutron intensities. From preliminary modeling conducted by the authors and R. Rosolem (personal communication, 2015) we believe that this missing correction will only have a minor effect on our results (Andreasen et al., 2016). Nevertheless, we suggest that future studies should investigate the effect of water vapor on thermal neutron intensities and develop appropriate correction methods.

2.2.2. Pure thermal and epithermal neutron detection

We expect thermal and epithermal neutrons to have unique responses to environmental properties and settings. Therefore, it is important to consider pure signals of thermal and epithermal neutrons, and not simply the raw neutron intensity signal measured by the bare and moderated detectors. In order to limit the epithermal and thermal neutron contribution to the bare and the moderated detectors, respectively, we use the cadmium-difference method (Knoll, 2010; Glasstone and Edlund, 1952). The thermal absorption cross-section of cadmium is very high (approximately 3500 barns) for neutron energies below 0.5 eV. The cross-section drops to approximately 6.5 barns at neutron energy 0.5 eV and remains low with increasing neutron energies. Thus, a cadmium shielded neutron detector only measures neutrons of energies higher than 0.5 eV. The epithermal neutron intensity was measured from a cadmium shielded moderated detector, while the thermal neutron intensity was calculated by subtracting the neutron intensity measured by the cadmium-shielded bare detector from the neutron intensity measured by the bare detector (unshielded). The cadmium-difference method is described in Andreasen et al. (2016) in detail.

Appropriate neutron energy correction models were applied in order to obtain pure thermal and pure epithermal neutron intensity measurements for the time periods when the cadmium-difference method was not applied (Andreasen et al., 2016). The neutron energy correction models were obtained from field campaigns applying the cadmium-difference method on bare and moderated detectors at various locations (height levels and land covers).

2.2.3. Footprint

The footprint of the bare detector is unexplained, while the footprint of the moderated detector was determined from modeling by Desilets and Zreda (2013) and Köhli et al. (2015). However, the findings of these two studies were inconsistent. Desilets and Zreda (2013) used the neutron transport code Monte Carlo N-Particle eXtended (MCNPx) and found the footprint to be nearly 600 m in diameter in dry air, while Köhli et al. (2015) using the Ultra Rapid Adaptable Neutron-Only Simulation (URANOS) estimated the footprint to be 260 – 480 m in diameter depending on the air humidity, soil moisture and vegetation. The potential mismatch in the footprint of the bare and the moderated detectors is a concern when combining the neutron intensity measurements. Nevertheless, the environmental conditions at the field sites are fairly homogeneous and although the footprint might be different we assume as a first approximation that the neutron intensity measured using the bare and the moderated detectors are comparable.

2.2.4. Field measurements

Three field sites are used in this study; the primary site is Gludsted Plantation, and two secondary sites are Voulund Farmland and Harrild Heathland. The three sites are all located within the Skjern River Catchment in the Western part of Denmark and represents the three major land use types (Figure 1) of the Danish hydrological observatory (HOBE) (Jensen and Illangasekare, 2011). The sites are situated at an elevation of approximately 50 - 60 m above sea level on an outwash plain from the last glaciation composed of nutrient depleted sandy stratified soils. Harrild Heathland is located 1 km south of Voulund Farmland, both approximately 10 km west of Gludsted Plantation.

Figure 1 is inserted here

Gludsted Plantation forest field site (56°04'24"N 9°20'06"E) is situated within a coniferous forest plantation covering an area of around 3500 ha. The trees of the plantation are densely planted in rows and are in general composed of Norway spruce with small patches of Sitka spruce, Larch and Douglas fir. Within the field site area (38 ha) the trees were estimated to be up to 25 m high and the dry above-ground biomass to be around 100±46 t/ha (one standard deviation) using LiDAR images from 2006 and 2007 (Nord-Larsen and Schumacher, 2012). The dry below-ground biomass was calculated to be 25 t/ha using a root-to-shoot ratio (the weight of the roots to the weight of the aerial part of the tree) for Norway spruce of 0.25 (Levy et al., 2004). Information on the vegetation at the forest field site (e.g. tree species, ages, heights and trunk diameters) is acquired from a register managed by the Danish Nature Agency (representative of the 2012 conditions); see Table 2.

Table 2 is inserted here

In Scandinavian forests around 79% of the total above-ground biomass of Norway spruce is stored within the tree trunks. The remaining 21% is found in the branches and needles (termed *foliage*). A typical density of the tree trunk is 0.83 g cm^{-3} (Serup et al., 2002). The major component of the tree biomass is cellulose ($C_6H_{10}O_5$) and represents around 55% of the total mass, while the remaining 45% is vegetation water (Serup et al., 2002). Based on these approximations, the wet above- and below-ground biomass at the field site area are estimated to be 182 t/ha and 45 t/ha, respectively. With a leaf area index

(LAI) of 4.5 and a canopy interception capacity coefficient of 0.5 mm/LAI (Andreasen et al., 2013) the maximum storage of canopy intercepted rain is estimated to be 2.25 mm.

Soil samples were collected within the footprint of the cosmic-ray neutron detector on August 26 – 27, 2013 following the procedure of Franz et al. (2012). Based on these samples the organic rich litter layer is found to be 5 - 10 cm thick. The dry bulk density of the litter and mineral layer are calculated by oven-drying the soil samples (Table 2), and the soil organic matter content of the mineral soil is determined from the loss-on-ignition method (16.9% in 10 - 20 cm depth and 7.6% in 20 - 30 cm depth). A time series of volumetric soil moisture is calculated from cosmic-ray neutron intensity, starting in spring, 2013, using the standard N_0-method as presented in Desilets et al. (2010). Lastly, the chemical composition of the soil matrix is estimated for two random soil samples collected at 20-25 cm depth using the *X-ray fluorescence* (XRF) analysis (Table 3).

Table 3 is inserted here

The element Gadolinium (Gd) can have a significant impact on thermal neutron intensity even at low concentrations due to its very high absorption cross-section of 49000 barns (1 barn = 10^{-24} cm^2). The detection limit of the XRF in this study is 50 ppm for Gd. The two soil samples from Gludsted Plantation both have Gd concentration below the detection limit of the XRF. Inductively coupled plasma mass spectrometry (ICP-MS) detects metals and several non-metals at very small concentrations and was used to characterize the soil chemistry of a nearby field site with similar soil conditions (Salminen et al., 2005). A Gd concentration of 0.51 ppm was found at that site and we assume this value to be representative of the conditions at Gludsted Plantation.

Gludsted Plantation is a heavily equipped research field site with a 38-m high tower for measurements at multiple heights within the forest canopy. At Gludsted Plantation, CR1000/B systems were installed at ground level (1.5 m height) and canopy level (27.5 m height) in the spring of 2013. Hourly neutron intensities have been continuously detected (Andreasen et al., 2016) except for short periods where the detectors were used for other types of measurements or during times of malfunctions. Neutron intensity profiles extending from the ground surface to 35-m-height above the ground were measured at approximately 5 m-increments during two field campaigns on November 28 – 29, 2013 and March 12 - 14, 2014. In order to obtain comparability between measurements and modeling pure thermal and epithermal neutron signals were estimated using neutron energy correction models on measurements from bare and moderated detectors, respectively. Both the time-series and neutron height profile measurements were corrected. Additionally, during the field campaign on March 12 -14, 2014 an epithermal neutron intensity profile (with no thermal contribution) was measured using a cadmium-shielded moderated detector (Andreasen et al., 2016). For the profile measurements neutron intensities were recorded at a 10-minute time resolution. As the thermal neutron intensity decreases significantly with height we choose to extend the time of measurement with the height level to maintain a low and consistent measurement uncertainty. The volumetric soil moisture estimated from the cosmic-ray neutron intensity (Zreda et al., 2008) was 0.18 m^3 m^{-3} during both field campaigns.

Voulund Farmland (56°02'14"N 9°09'38"E) is an agricultural field site. In 2015, the fields were cropped with spring barley. After harvest in the late summer until ploughing in spring 2016 (prior to sowing) the fields were covered with stubble (around 10 cm high). A 25 cm layer of relatively organic rich soil (4.45% soil organic matter) is found at the top of the soil column and is a result of the cultivation practices. More information about the field site can be found in Andreasen et al. (2016). Ground level neutron intensities were measured on September 22 and 23, 2015 at Voulund Farmland (Andreasen et al., 2016). The measurements were conducted using the bare and the moderated neutron detectors normally installed at Gludsted Plantation and data were logged every 10 minutes. In order to obtain pure thermal and epithermal neutron intensities the neutron energy correction models were applied.

Harrild Heathland (56°01'33"N 9°09'29"E) is a shrub land field site dominated by grasses and heather. The heathland is maintained by controlled burning, yet, the field site area has not recently been burnt. The organic rich litter layer is found to be around 10 cm thick during soil sampling field campaigns at the field site. Due to podsolization a low permeable hardpan-layer hindering percolation to deeper depths is present at around 25-30 cm depth. In the period from October 27 to November 16, 2015 the ground level thermal and epithermal neutron intensity was measured directly at Harrild Heathland using the cadmium-difference method (Knoll, 2010). The cadmium-difference method was applied using two bare and one moderated detector normally installed at Gludsted Plantation. The neutron intensity was integrated and recorded on an hourly basis.

2.3. Neutron transport modeling

The three-dimensional Monte Carlo N-Particle transport code version 6 (MCNP6) (Pelowitz, 2013) simulating thermal and epithermal neutrons is used to model the forest field site. The code holds libraries of measured absorption and scattering cross-sections used to compute the probability of interactions between earth elements and neutrons. The MCNP6 combines Monte Carlo N-Particle Transport code version 5 (MCNP5) and Monte Carlo N-Particle Extended Radiation Transport code (MCNPX). MCNPX has been used for most neutron transport modeling within the field of hydrology (Desilets et al., 2013; Rosolem et al., 2013; Zweck et al., 2013). However, the improved and more advanced MCNP6 has recently been introduced. This updates version provided more realistic neutron intensity profiles for Voulund Farmland field site (Andreasen et al., 2016).

The number of particle histories released at the center of the upper boundary of the model domain is specified to obtain an uncertainty below 1%. The released particles represent a distribution of high-energy particles typical for the spectrum of incoming cosmic-rays traveling through the atmosphere. The modeled neutron intensities are normalized per unit source particle providing relative values (Zweck et al., 2013). In order to obtain values comparable to measurements conversion factors are used (Andreasen et al., 2016). The conversion factors 3.739×10^{12} and 1.601×10^{13} are multiplied by the modeled thermal neutron fluences in the energy range of 0 – 0.5 eV and epithermal neutron fluences in the energy range 10 – 1000 eV, respectively. We stress that, the conversion factors are detector-specific as well as dependent on the horizontal area of the model-setup in MCNP6.

2.3.1. The Gludsted Plantation reference model

The model domain of MCNP6 is defined by cells of varying geometry, and each cell is assigned a specific chemical composition and density. The lowest 4 m of the Gludsted Plantation reference model consists of subsurface layers. The chemical composition of the mineral soil is prescribed according to the chemical composition from XRF measurements; assumed Gd concentration of 0.51 ppm, wet below-ground biomass (cellulose) of 45 t/ha, dry bulk density of 1.09 g cm^{-3} and volumetric soil moisture content of 0.18 m^3 m^{-3}. The litter layer is defined according to the chemical composition of cellulose, dry bulk density of 0.34 g cm^{-3} and moisture content similar to that of mineral soil (see also Table 3). The same volumetric soil moisture was used for the whole soil column, as the volumetric soil moisture profile was unknown for the days of neutron profile measurements. The atmosphere is composed of 79% nitrogen and 21% oxygen by volume and extends from the forest canopy surface to the upper boundary of the model domain at approximately 2 km height. Here, an incoming spectrum adapted to the specific level of the atmosphere is specified (Hughes and Marsden, 1966). The density of air is assumed to be 0.001165 g cm^{-3}. Throughout the domain multiple sublayers of varying vertical discretization cover the vertical extent of the model in order to record neutron intensities at multiple heights and depths from the ground surface. The thickness of the layers decreases with proximity to the ground surface ranging in thickness from 0.025 m to 0.20 m for the subsurface layers and from 1 m to 164 m for the layers above the ground surface. The neutron intensity detectors are represented by 1-m-high layers extending the full lateral model domain (400 m x 400 m) and are used from the ground to 28 m height corresponding to the measured heights. Reflecting surfaces constrain the model domain. Thus, the particles reaching a model boundary will be reflected specularly back into the model domain. Wet above-ground biomass of 182 t/ha is distributed homogeneously within the forest canopy layers, i.e., from the ground surface to 25 m above the ground (Table 4).

The proper way to conceptualize the forest canopy in the model-setup is not obvious and the sensitivity to forest representation on neutron intensity is therefore investigated using four model-setups of increasing complexity. In the first representation (Model *Foliage*; Figure 2B) the same material composed of cellulose and air (foliage) is assigned all forest canopy layers. In order to obtain a wet above-ground biomass of 182 t/ha a relatively low density of 0.00189 g cm^{-3} is calculated for the material. In order to allow for a forest canopy layer to be composed of multiple materials (cellulose and air) and densities (massive tree trunks and less dense foliage and air), the horizontal discretization of the forest canopy layers is reduced to smaller cells for the next tree model-setups. The bole of each tree is for all three model-setups represented by a cylinder with a diameter of 0.14 m, a composition of cellulose, and a density of 0.83 g cm^{-3}. A tree is placed at the center of each cell and extends from the ground surface to the top of the forest canopy layer. In the second representation (Model *Tree trunk, Air*; Figure 2C) the horizontal discretization of the forest canopy layers is set to 4.20 m by 4.20 m and the remaining volume beyond the bole of the tree consist of air alone (density 0.001165 g cm^{-3}). Thus, for this model all biomass is stored in the bole of the trees and the cell size is adjusted to obtain a wet above-ground biomass of 182 t/ha resulting in 9070 trees within the model domain. In the third representation (Model *Tree trunk, Foliage*; Figure 2D) the horizontal discretization of the forest canopy layers is 4.72 m by 4.72 m and the remaining volume beyond the bole of the tree is made of foliage. As previously described, the share of biomass stored in the tree trunk and the foliage is 79% and

21%, respectively, typical of Norway spruce. The foliage material is a composite of cellulose and air and the density is the sum of the two (0.001318 g cm^{-3}). A total of 7182 trees are evenly spaced within the model domain. The fourth and most complex forest canopy conceptualization (Model *Tree trunk, Foliage*; Figure 2E) is equal to the Model *Tree trunk, Foliage* except that air is also included in the description of the forest canopy layers and the density of the foliage is increased to obtain the same above-ground biomass as for the other models. The foliage is specified as a 1.7 m thick band around the tree cylinder and the density of foliage material composed of air and cellulose is 0.00151 g cm^{-3}.

Table 4 and Figure 2 are inserted here

2.3.2. Sensitivity to environmental conditions

The sensitivity of thermal and epithermal neutron intensities to volumetric soil moisture is examined using modeling. The volumetric soil moisture in the Gludsted Plantation reference model is specified to 0.18 m^3 m^{-3} and both drier and wetter soils are modeled to test the sensitivity, i.e. 0.05 m^3 m^{-3}, 0.10 m^3 m^{-3}, 0.25 m^3 m^{-3}, 0.35 m^3 m^{-3} and 0.45 m^3 m^{-3}. The forest canopy conceptualizations of Model *Tree trunk, Foliage, Air* and Model *Foliage* are used.

The thermal and epithermal neutron intensity is a product of hydrogen abundance as well as elemental composition. The Gludsted Plantation reference model with the complex forest conceptualization (Model *Tree trunk, Foliage, Air)* is used to test the sensitivity of thermal and epithermal neutron intensities to soil chemistry. It holds the most complex soil chemistry (*fourth order complexity*) with multiple subsurface layers composed of measured concentrations of major elements determined by XRF, soil organic matter, gadolinium and roots (Table 3). In order to test the effect of simplifying the soil chemistry a component is excluded one at the time: 1) *third order complexity*; soil organic matter is excluded, 2) *second order complexity*; soil organic matter and roots are excluded, 3) *first order complexity*; soil organic matter, roots and gadolinium are excluded, and 4) *pure* SiO_2; all other components are excluded.

The sensitivity of the modeled thermal and epithermal neutron intensities to the presence of the organic litter layer is investigated using the Gludsted Plantation reference model with the complex forest conceptualization (Model *Tree trunk, Foliage, Air)*, in which the thickness of the litter layer is set to be 10.0 cm. Sensitivity simulations are carried out for the following thicknesses of the litter layer: 0.0 cm, 2.5 cm, 5.0 cm and 7.5 cm. For all litter layer models, the total thickness of the subsurface is kept constant at 4 m.

The materials of forest floor litter and mineral soil differ distinctly in terms of chemical composition and dry bulk density. The determination of dry bulk density of the two materials is characterized by high measurement uncertainty, especially for the litter as sampling and drying is very challenging for materials including large amounts of soil organic matter (O'Kelly, 2004). Given that the elemental composition and density of the soil matrix is relevant for the neutron intensity the sensitivity of dry bulk density on thermal and epithermal neutron intensity is examined. The dry bulk density of the Gludsted Plantation reference model is 0.34 g cm^{-3} for the litter layer and 1.09 g cm^{-3} for the mineral soil. The Gludsted Plantation reference model with the complex forest conceptualization (Model *Tree trunk, Foliage, Air)* is used to test the sensitivity applying four scenarios: 1) higher dry bulk density of the litter layer (0.50 g cm^{-3}), 2) higher dry bulk density of

the mineral soil (1.60 g cm^{-3}), 3) lower dry bulk density of the litter layer (0.20 g cm^{-3}), and 4) lower dry bulk density of the mineral soil (0.60 g cm^{-3}). All values with the exception of higher dry bulk density of 1.60 g cm^{-3} for the mineral soil (standard value for quartz; soil particle density of 2.66 g cm^{-3} and a porosity of 0.40) are within the range of the measurements at the site (see Table 2).

The Gludsted Plantation reference model with the complex forest conceptualization (Model *Tree trunk, Foliage, Air)* is used to test the sensitivity to canopy interception by increasing the density and water content of the cells described by foliage material. The forest canopy of the reference model is dry (foliage material density 0.00151 g cm^{-3}). In order to test the effect, water equivalent to 1 mm (foliage material density 0.00155 g cm^{-3}), 2 mm (foliage material density 0.00159 g cm^{-3}) and 4 mm (foliage material density 0.00167 g cm^{-3}) of canopy interception is added to the foliage volume. This changes both the wet bulk density and the atomic fraction of the foliage material.

The sensitivity to biomass is investigated using the Gludsted Plantation reference model with the complex forest conceptualization (Model *Tree trunk, Foliage, Air*) and the simplified model-setup (Model *Foliage*). The biomass of the Gludsted Plantation reference model is equivalent to a dry above-ground biomass of 100 t/ha and a dry below-ground biomass of 25 t/ha, following the root-to-shoot ratio of 0.25 typical of Norway spruce. This distribution is used for both model setups. For the sensitivity analysis one model without vegetation (Model *0 t/ha*, Figure 2A) and three models with different amounts of biomass are used (see Table 4). The forest canopy layer extending uniformly from the ground to 25 m above the ground surface is for the model with no vegetation assigned with the material composition and density of air. The amount of biomass modeled for the three remaining models is equivalent to a dry above-ground biomass of: 1) 50 t/ha, 2) 200 t/ha, and 3) 400 t/ha. The size of the cells in the forest layers and the density of the foliage material are adjusted in order to obtain the correct amount of biomass.

3. Results

3.1. Gludsted Plantation

The neutron intensity profiles for Gludsted Plantation are modeled using four different forest canopy conceptualizations. The model results are presented in Fig. 3 along with time-series of hourly and daily ranges of thermal and epithermal neutron intensities collected at the Gludsted Plantation during the period 2013-2015, and measured/estimated thermal and epithermal neutron intensity profiles (November 2013 and March 2014). Note that a decrease in the epithermal neutron intensity from the ground level to 5 m above the ground surface was measured in March 2014. This is in disagreement with theory (see Section 2.1.) and is expected to be a result of measurement uncertainties. Following the Poissonian statistics the relative uncertainty decreases with increasing neutron intensity. The relative measurement uncertainty is therefore higher for the hourly time series data than for the multi-hourly (2-12 hours) and daily measurements. Accordingly we choose to rely mostly on the daily averages of time-series measurements.

Figure 3 is inserted here

Overall, time-series and profile measurements provide similar results in agreement with theory. The thermal neutron intensity decreases considerably with height above ground surface and is at canopy level reduced by around 50% compared to at the ground level. The epithermal neutron intensity increases slightly with height and is around 10-15% higher at the canopy level compared to the ground level. Overall, a remarkable agreement between measured and modeled neutron intensities is seen in Fig. 3. We stress that no calibration of the governing physical properties in the forest model is performed and that the estimates are based on measured properties. The ground and canopy level thermal and epithermal neutron intensity for the four forest canopy conceptualization models are provided in Table 5. All modeled neutron intensity profiles are within the range of hourly time-series measurements, and in particular the thermal neutron profiles are in agreement with measurements. The models of the more complex forest canopy conceptualizations, including a tree trunk, provide similar thermal and epithermal neutron profiles. The ground and canopy level thermal neutron intensity of models with forest canopy conceptualization of Model *Tree trunk, Foliage* and Model *Tree trunk, Foliage, Air* are within the daily ranges of the time-series measurements. In contrast, the modeled epithermal neutron profiles of the more complex models are slightly underestimated and the profile slope is steeper than the measured profiles. Nevertheless, the modeled epithermal neutron intensity profile is still within the ranges of the time-series of hourly measurements at both height levels. The neutron intensity profiles of the simpler forest canopy conceptualization of Model *Foliage* is less steep and is the only model providing an epithermal neutron intensity profile within the daily ranges of the time-series measurements at both the ground and canopy level. All in all, then compared to the range of daily time-series measurements, the best fit of the thermal measurements is found using a more complex conceptualization, while the simple foliage conceptualization matches the epithermal measurements better.

Table 5 is inserted here

In this study, a sensitivity analysis is performed using the most complex model to examine the effect of soil moisture, soil dry bulk density and composition, litter and mineral soil layer thickness, canopy interception and biomass on the thermal and epithermal neutron transport at the immediate ground-atmosphere interface. Since the most appropriate forest canopy conceptualization is not obvious from Fig. 3 the simplest forest canopy conceptualization was also used to examine the effect of soil moisture and biomass on the neutron transport.

3.2. Soil moisture

The modeled thermal and epithermal neutron intensity profiles of Model *Tree trunk, Foliage, Air* and Model *Foliage* using six different volumetric soil moistures, 0.05 $m^3\ m^{-3}$, 0.10 $m^3\ m^{-3}$, 0.18 $m^3\ m^{-3}$, 0.25 $m^3\ m^{-3}$, 0.35 $m^3\ m^{-3}$ and 0.45 $m^3\ m^{-3}$, are presented in Figs. 4 and 5, respectively. To enable comparison the measurements included in Fig. 3 are also included in Figs. 4 and 5. The sensitivity of soil moisture on thermal and epithermal neutron intensities at the ground and canopy level relative to the Model *Tree trunk, Foliage, Air* and Model *Foliage* at reference conditions (volumetric soil moisture 0.18 $m^3\ m^{-3}$) is provided in Table 6.

Figure 4, Figure 5 and Table 6 are inserted here

As expected, the thermal and epithermal neutron intensity decreases with increasing soil moisture (Table 6, Figs. 4 and 5). For both model-setups, the largest changes in neutron intensity occur at the dry end of the soil moisture range and for the epithermal neutrons. For Model *Tree trunk, Foliage, Air* (Figure 4), only a minor decrease in the sensitivity of soil moisture on epithermal neutron intensity is observed going from ground level to canopy level (approximately 15% reduction in intensity range corresponding to a volumetric soil moisture change of 0.40 m^3 m^{-3}). On the other hand, the sensitivity of the thermal neutron intensity is reduced more than 50% (Table 6) most likely caused by the lower mean-free path length of the thermal neutrons compared to that of epithermal neutrons. The model with a simple forest canopy conceptualization provides thermal and epithermal neutron intensities slightly more sensitive to soil moisture (Figure 5). Neutron intensity at dry and wet soil conditions is represented by the range of time-series neutron intensity measurements. Overall, the modeled neutron intensities are within the measurement range and the more appropriate model-setup for Gludsted Plantation is not obvious from the modeling results.

3.3. Subsurface properties

Thermal and epithermal neutron intensity profiles are modeled using Model *Tree trunk, Foliage, Air* (with *fourth order complexity*) and models of decreasingly complex soil. Soil organic matter, below-ground biomass, Gd and the chemical composition from XRF measurements are excluded one at the time (from *third* to *first order complexity*) and the final model includes a simple silica soil (SiO_2). The exact sensitivity of excluding the different components on ground and canopy level thermal and epithermal neutron intensity is quantified in Table 6 (see values in parentheses). Only the removal of soil organic matter (*third order complexity*) changes the neutron intensity significantly at Gludsted Plantation, i.e. an increase in the ground level thermal and epithermal neutron intensity of 19 cts/hr (cts = counts) and 25 cts/hr, respectively, is observed.

The thermal and epithermal neutron intensity is also modeled for a forest with litter layer of various thicknesses (Figure 6A). The Model *Tree trunk, Foliage, Air* including a 10.0 cm thick litter layer is used along with forest models with litter layers of 0.0 cm, 2.5 cm, 5.0 cm and 7.5 cm thickness.

Figure 6 is inserted here

Neutron intensities are found to decrease with an increasing layer of litter, having the greatest impact on the epithermal neutron intensities (see also Table 6). Thereby, the thermal-to-epithermal neutron (t/e) ratio is altered when changing the thickness of the litter layer. This effect is most pronounced when the model without a litter layer is compared to the model with just a thin 2.5 cm thick litter layer. Since a considerable range of dry bulk density values (see Table 2) is measured within the footprint of the neutron detector the sensitivity of neutron intensity to litter and mineral soils dry bulk density is examined using four model setups. Relative to the Gludsted Plantation reference model higher and lower values of dry bulk density are used. The first model includes a higher dry bulk density of 0.50 g cm^{-3} for the litter layer, while the second model holds a higher dry bulk density of 1.60 g cm^{-3} for the mineral soil. The third model has a low dry bulk density of 0.20 g cm^{-3} specified for the litter layer, and in the fourth model the mineral soil is described by a low dry bulk density of 0.60 g cm^{-3}. The four model setups only provided slightly different thermal and epithermal neutron intensities (Table 6). Nevertheless, a reverse response of changed bulk densities is observed. A decrease in neutron intensity is obtained both by

increasing the dry bulk density of the litter material and decreasing the dry bulk density of the mineral soil. Conversely, higher neutron intensities are computed by decreasing the dry bulk density of the litter material and increasing the dry bulk density of the mineral soil.

3.4. Canopy interception

The effect of canopy interception on thermal and epithermal neutron intensity is modeled using Model *Tree trunk, Foliage, Air* (Figure 6B and Table 6). Except for a slight increase in ground level thermal neutron intensities with wetting of the forest canopy, no effect of canopy interception on ground and canopy level thermal and epithermal neutron intensity is observed. A maximum change of approximately 3% (15 cts/hr) is observed for thermal neutron intensity at ground level going from a dry canopy to 4 mm of canopy interception. At the specific field site a maximum canopy storage capacity of 2.25 mm is expected, producing a change in observed ground level thermal neutron intensity of approximately 7 cts/hr. Given an average neutron intensity of 504 cts/hr of ground level thermal neutrons with the installed detectors, an uncertainty of 22 cts/hr is expected based solely on Poissonian statistics (see Section 2.2.1.). Thus, the signal of canopy interception is within the measurement uncertainty, and cannot be identified at Gludsted Plantation using the available cosmic-ray neutron measurements.

Although detection of canopy interception at Gludsted Plantation is unfavorable it may still be possible at more appropriate conditions. Canopy interception modeling as described above is therefore also performed for volumetric soil moisture 0.05 $m^3\ m^{-3}$, 0.10 $m^3\ m^{-3}$, 0.25 $m^3\ m^{-3}$ and 0.40 $m^3\ m^{-3}$. Ground level t/e ratio of the 20 model combinations are plotted against ground level thermal neutron intensity, ground level epithermal neutron intensity and volumetric soil moisture (Figure 7). We chose not to include measurements in the figure because the measurement uncertainty at a relevant integration time is greater than the signal of canopy interception.

Figure 7 is inserted here

Overall, ground level t/e ratio is found to be independent of ground level thermal neutron intensity (Figure 7A), ground level epithermal neutron intensity (Figure 7B) and volumetric soil moisture (Figure 7C). Furthermore, the ground level t/e ratio is found to increase with increasing canopy interception being on average 0.804 and 0.836 for a dry canopy and 4 mm of canopy interception, respectively. Overall, the same increase in ground level t/e ratio is obtained per 1 mm additional canopy interception.

3.5. Biomass

The sensitivity to the amount of forest biomass on thermal and epithermal neutron intensity using the forest canopy conceptualization of Model *Tree trunk, Foliage, Air* and Model *Foliage* are presented in Fig. 6C and Fig 6D, respectively. The neutron intensity is provided for a scenario with no vegetation and models with biomass equivalent to dry above-ground biomass of: 50 t/ha, 100 t/ha (Gludsted Plantation), 200 t/ha and 400 t/ha.

Forest biomass is seen to significantly alter the thermal and epithermal neutron intensity both with regards to the differences between ground and canopy level neutron intensity, and ground level t/e ratios (Figures 6C and 6D). The direction and magnitude of these changes are found to be different depending on the two forest canopy conceptualizations. For the Model *Tree trunk, Foliage, Air* the increase in biomass results in an increase in thermal neutron intensity while the epithermal neutron intensity decreases (Figure 6C). From ground level and up to an elevation of approximately 20 m the sensitivity to the amount of biomass on the neutron intensity is almost the same. From 20 m height, the sensitivity decreases with increasing elevation and for thermal neutrons the signal of biomass is almost gone at canopy level (not presented here). At canopy level, the sensitivity on epithermal neutrons is reduced, yet, a strong signal remains.

Increasing the biomass in the Model *Foliage* from 0 t/ha to 50 t/ha (Figure 6D) results in a considerable increase in ground level thermal neutron intensity (136 cts/hrs, Table 6) while at canopy level thermal neutron intensity is almost unaltered. A further increase in biomass (>50 t/ha) decreases both ground and canopy level thermal neutron intensities. The epithermal neutron intensity decreases at ground level and increase proportionally at canopy level with increasing amounts of biomass. The epithermal neutrons produced in the ground escape to the air and are moderated by the biomass, resulting in reduced epithermal neutron intensity with greater amounts of biomass. All models provide in accordance to theory increasing epithermal neutron intensity with height, yet, the reduced steepness of the neutron height profiles with added biomass is unexplained. Oppositely to Model *Tree trunk, Foliage, Air*, the ground level thermal neutron intensity decreases with added biomass.

As shown in Figs. 3, 6C and 6D the resulting thermal and epithermal neutron intensity profiles depend highly on the chosen model-setup (forest conceptualization). At this stage, we cannot determine which conceptualization is more realistic, and we therefore choose to use both conceptualizations in the further analysis. Overall, a positive correlation is found for the differences between ground and canopy level neutron intensity (thermal and epithermal neutron energies) and the amount of biomass (Figures 6C and 6D, and Table 6). However, the Model *Tree trunk, Foliage, Air* and Model *Foliage* provide different relationships, and measurements and modeling are not fully in agreement. Alternatively, one can also potentially use the t/e ratio at the ground level to assess biomass. The advantage is that only one station is needed - and that at a convenient location. This would also allow for surveys of biomass estimations to be conducted from mobile cosmic-ray neutron intensity detector systems, e.g. installed in vehicles.

The measured and modeled ratios are again provided using both forest canopy conceptualization, i.e. Model *Tree trunk, Foliage, Air* (Figure 8) and Model *Foliage* (Figure 9). The ratios are plotted against A) ground level thermal neutron intensity, B) ground level epithermal neutron intensity, and C) volumetric soil moisture estimated using the N_0-method (Desilets et al., 2010). Measurements are provided as daily averages, biweekly averages and as a total average of the whole two-year-period.

Figure 8 and Figure 9 are inserted here

The modeled ground level t/e ratio increases with forest biomass (Figures 8 and 9). Drying or wetting of soil change the thermal and epithermal neutron intensity proportionally and the ratios are accordingly found to be independent of changes in the ground level thermal neutron intensity, the ground level epithermal neutron intensity and volumetric soil moisture. However, this independence is not seen in the measurements, where the ground level epithermal neutron intensity and soil moisture (Figures 8C and 9C) in particular seem to impact the ratio. A fairly proportional increase in the ground level t/e ratio with respect to greater amounts of biomass is found when using Model *Tree trunk, Foliage, Air* (Figures 8 and 10). Contrarily, when using Model *Foliage*, a more uneven increase in the ratio with increasing amounts of biomass is provided (Figures 9 and 10). A major increase in the ground level t/e ratio of around 0.22 appears from no vegetation to a dry above-ground biomass of 50 t/ha. However, additional amounts of biomass only increase the ground level t/e ratio slightly. With additional 350 t/ha biomass (from 50 t/ha to 400 t/ha dry above-ground biomass) the t/e ratio increases by only 0.05.

Figure 10 is inserted here

Overall, a remarkable agreement is seen for the Model *Tree trunk, Foliage, Air* in Fig. 8 when comparing the two-year-average of the measured ratio with the modeled value of Gludsted Plantation (100 t/ha dry above-ground biomass, Figure 8). The biweekly averages of measurements are all within the ratios modeled for biomass of 50 t/ha - 200 t/ha. For the Model *Foliage* in Fig. 9 the measured ratio is in better agreement with a lower biomass (50 t/ha dry above-ground biomass). The small increase in t/e ratio with increasing amounts of biomass of Model *Foliage* causes the biweekly averages of the measurements to exceed both the lower and upper boundary of ratios provided by the models of 50 t/ha and 400 t/ha dry above-ground biomass.

4. Discussions

4.1. Neutron height profile measurements and forest conceptualization

Slightly different neutron height profiles and t/e ratios were measured during the field campaigns in November 2013 and March 2014 (Figures 3-5). The area average soil moisture estimated using the measured cosmic-ray neutron intensity was similar for the two field campaigns. The different neutron height profiles could therefore instead be a result of dissimilar soil moisture profiles or different soil moisture of the litter layer and the mineral soil. During two out of three soil sampling field campaigns different soil moisture of the litter layer and the mineral soil was observed at Gludsted Plantation (soil samples were collected at 18 locations within a circle of 200 m in radius and in 6 depths from 0-30 cm depth following the procedure of Franz et al. (2012)). Additionally, the different neutron height profiles could also be a result of the different climate and weather conditions related to the seasons of detections (spring and fall). However, both neutron profiles are within the ranges of the daily time-series measurements and we therefore still believe that they can be used in the assessment of the modeled neutron profiles. For future studies we recommend soil sample field campaigns to be conducted on the days of neutron profile measurements.

The neutron transport at the ground-atmosphere interface was found to be sensitive to the level of complexity of the forest canopy conceptualization, yet, the more appropriate conceptualization was not identified. Improved comparability to measurements may be obtained by advancing the forest canopy conceptualization. Currently, one tree is defined and repeated throughout the model domain. The trees are placed in rows and the same settings are applied from the ground surface to 25 m height. In order to advance the forest canopy conceptualization, trees of different heights and diameters could be included, and the placement of the trees could be more according to the actual placement of trees at the forest field site. Additionally, variability in tree trunk diameter, foliage density and volume with height above the ground surface could be implemented.

4.2. The sensitivity of neutron intensity to soil chemistry and dry bulk density

In contrary to the results obtained at Voulund Farmland by Andreasen et al. (2016), the sensitivity of thermal and epithermal neutron intensity profiles to soil chemistry was found to be minor at Gludsted Plantation. The soil organic matter content at Voulund Farmland is smaller and the soil chemistry is, except from a few elements (added in relation to farming activities; spreading of manure and agricultural lime), similar to Gludsted Plantation. Modelling shows that the sensitivity to soil chemistry at Gludsted Plantation is dampened by the considerable amount of hydrogen present in the litter at the forest floor and the forest biomass (not presented here). Accordingly, the effect of litter and mineral soil dry bulk density on neutron intensity is expected to be greater at non-vegetated field site. The reverse effect of increased dry bulk density of litter and mineral soil on neutron intensity is a result of the different elemental composition of the two materials. The production rate of low energy neutrons (<1 MeV) per incident high-energy neutron is higher for interactions with elements of higher atomic mass ($A^{2/3}$, where A is the atomic mass) (Zreda et al., 2012). Heavier elements are in particular found in mineral soil and an increase in the dry bulk density entails a higher production rate and therefore higher neutron intensity. The concentration of hydrogen is increased with an increased dry bulk density of litter material resulting in a greater moderation and absorption of neutrons, and as a consequence lower neutron intensities. To summarize, the mineral soil acts as a producer of thermal and epithermal neutrons, while the litter acts as an absorber.

4.3. The potential of cosmic-ray neutron canopy interception detection

Ground level thermal neutron intensity was found to be sensitive to canopy interception, however, the signal is small and within the measurement uncertainty at Gludsted Plantation. In order to obtain a signal-to-noise ratio of 1, either an 11-hour-integration time or 11 detectors similar to the installed detector are needed. However, longer integration times are not appropriate when considering Gludsted Plantation as the return time of canopy interception (cycling between precipitation and evaporation) often is short (half-hourly to hourly time resolution). Although the change in the t/e ratio with wetting/drying of the forest canopy is small the canopy interception may potentially be measured using cosmic-ray neutron intensity detectors at locations with: 1) a high neutron intensity level (lower latitude and/or higher altitude, 2) more sensitive neutron detectors, and 3) greater amounts of canopy interception with longer residence time (e.g. snow). We suggest future studies investigating the effect of canopy interception on the neutron intensity signal to be performed at locations matching one or more of these criteria.

4.4. The sensitivity of biomass to neutron intensity

The neutron intensity depends on how many neutrons are produced, down-scattered to lower energies and absorbed. Including biomass to a system increases the concentration of hydrogen and leads to reduced neutron intensity as the moderation and absorption is intensified. Despite this, increased thermal neutron intensity is provided with greater amounts of forest biomass using Model *Tree trunk, Foliage, Air* (see Figure 6C). We hypothesize that forest biomass enhances the rate of moderation more than the rate of absorption. Thus higher thermal neutron intensity is obtained as the number of thermal neutrons generated by the moderation of epithermal neutrons exceeds the number of thermal neutrons absorbed. This behavior may be due to the large volume of air within the forest canopy. The probability of thermal neutrons to interact with elements within this space is low as the density of air is low. Overall when applying Model *Foliage* both thermal and epithermal neutron intensity decreases with added amounts of biomass (see Figure 6D). The deviating behavior (compared to Model *Tree trunk, Foliage, Air*) may be due to the different elemental concentration of the forest canopy layers. Here, no space is occupied by a material of very low elemental density and may lead to an increased absorption of thermal neutrons.

The discrepancy of measured and modeled ground level t/e ratios (Figures 8 and 9) could be related to: 1) shortcomings in the model setup, i.e. a need for an even more realistic forest conceptualization, and more detailed and up-to-date forest information. A model including a sufficient representation of the field site will provide neutron height profiles and t/e ratios more representative of the real conditions, 2) discrepancy of measured and modeled energy ranges as discussed in Andreasen et al. (2016), and 3) unrepresentative biomass estimate. The 100 t/ha dry above-ground biomass was estimated using LiDAR images from 2006 and 2007 and therefore not completely representative of the 2013-2015 conditions (because of tree growth). Furthermore, the biomass estimate varied considerably within the image (standard deviation = 46 t/ha), and the image coverage did not fully match the footprint of the cosmic-ray neutron intensity detector.

4.5. Cosmic-ray neutron biomass detection

The proposed possibility of estimating biomass at a hectometer scale using ground level t/e ratios was tested. The modeled ground level t/e ratio is compared with measurements of two additional field sites located close to Gludsted Plantation. The three field sites have similar environmental settings (e.g. neutron intensity, soil chemistry), though different land covers with different amounts of biomass (stubble pasture, heathland and forest).

At Voulund Farmland the ground level t/e ratio was measured to be 0.53 and 0.58 on September 22nd and September 23rd 2015, respectively. Only minor amounts of organic matter were present in the stubble and residual of spring barley harvested in August 2015. Additionally, the ground level t/e ratio was determined based on modeling of bare ground and site specific soil chemistry measured at Voulund Farmland (Andreasen et al., 2016). The modeled ratio was found to be 0.56 in agreement with the measured ratios. The ratio modeled based on the non-vegetated conceptualization of Gludsted Plantation was slightly higher (0.60, see Figures 8 and 9). Here, a 10 cm thick litter layer was included in the model. The sensitivity analysis on the effect of litter layer on neutron intensity (Figure 6A and Table 6) implies that lower ground level t/e ratios are found at locations with a thin or no litter layer.

The ground level t/e ratio at the Harrild Heathland was measured to 0.66 during the period October 27 to November 16 2015. The ratio is slightly higher than the non-vegetated model for Gludsted Plantation. Both field sites have a considerable layer of litter, and the slightly higher t/e ratio relative to the non-vegetated Gludsted Plantation may be due to biomass in the form of grasses, heather plants and bushes present at Harrild Heathland. At Gludsted Plantation, the ratio is 0.73 for dry above-ground biomass equivalent of 50 t/ha. Accordingly, the ratio measured at Harrild Heathland is somewhere in between the ratio modeled for a non-vegetated field site and a field site with biomass equivalent to 50 t/ha dry above-ground biomass.

Measuring ground-level t/e ratios for biomass estimation at a hectometer scale is promising as the measured ratio increases with increasing amounts of litter and biomass in correspondence to modeling. Still, ground level t/e ratio detection at locations of known biomass should be accomplished to test the suggested relationships. We recommend a detection system with higher sensitivity to be used when a location of low neutron intensity rates (like Gludsted Plantation) is surveyed, unless long periods of measurements can be conducted at each measurement location. This can be accomplished by using larger sensors, an array of several sensors and/or sensors that are more efficient, as is done in roving surveys (Chrisman and Zreda, 2013; Franz et al., 2015).

5. Conclusion

The potential of applying the cosmic-ray neutron intensity method for other purposes than soil moisture detection was explored using profile and time-series measurements of neutron intensities combined with neutron transport modeling. The vegetation and subsurface layers of the forest model-setup were described by average measurements and estimates. Four forest canopy conceptualizations of increasing complexity were used. Without adjusting parameters and variables, modeled thermal and epithermal neutron intensity profiles compared fairly well with measurements, yet, some deviations from measurements were observed for each of the four forest canopy conceptualization models. The more appropriate forest canopy conceptualization was not obvious from the results as the best fit to thermal neutron measurements was found using complex forest canopy conceptualization, including a tree trunk and multiple materials, while the better fit to epithermal neutron measurements was found using the simplest forest canopy conceptualization, including a homogenous layer of foliage material. A sensitivity analysis was performed to quantify the effect of the forest´s governing parameters/variables on the neutron transport profiles. The sensitivity of canopy interception, dry bulk density of litter and mineral soil, and soil chemistry on neutron intensity was found to be small. The ground level t/e neutron ratio was found to increase with increasing amounts of canopy interception and to be independent of ground level thermal neutron intensity, ground level epithermal neutron intensity and soil moisture. However, the increase was minor and the measurement uncertainty was found to exceed the signal of canopy interception at a timescale appropriate to detect canopy interception at Gludsted Plantation (half-hourly to hourly). Neutron intensity was found to be more sensitive to litter layer, soil moisture and biomass at the forest field site. An increased litter layer at the forest floor resulted in reduced neutron intensities, particularly for epithermal neutrons. Forest biomass was found to alter the thermal and epithermal neutron transport significantly, both in terms of the shape of the neutron profiles and the t/e neutron ratios. The response to altered amounts of biomass on thermal

and epithermal neutron intensity is non-unique for the simple and complex forest conceptualization and further advancement of the forest representation is therefore necessary. Still, cosmic-ray neutron intensity detection for biomass estimation at an intermediate scale is promising. Both the difference between ground and canopy level thermal and epithermal neutron intensity, respectively, and the ground level t/e ratios were found to increase with additional amounts of biomass using the simple and complex forest canopy conceptualization. The best agreement between measurements and modeling was obtained for the ground level t/e neutron ratio using a model with a complex forest canopy conceptualization. Additionally, the modeled ratios were found to agree well with two nearby field sites with different amounts of biomass (a bare ground agricultural field and a heathland field site).

6. Acknowledgements

We acknowledge The Villum Foundation (www.villumfonden.dk) for funding the HOBE project (www.hobe.dk). Lars M. Rasmussen and Anton G. Thomsen (Aarhus University) are greatly thanked for the extensive help in the field. We would like to extend our gratitude to Vivian Kvist Johannsen and Johannes Schumacher from the Section for Forest, Nature and Biomass, University of Copenhagen. Finally, we also acknowledge the NMDB database (www.nmdb.eu), founded under the European Union's FP7 programme (contract no. 213007) for providing data. Jungfraujoch neutron monitor data were kindly provided by the Cosmic Ray Group, Physikalisches Institut, University of Bern, Switzerland.

Reference

Andreasen, M., Jensen, K. H., Zreda, M., Desilets, D., Bogena, H. and Looms, M. C: Modeling cosmic ray neutron field measurements. Water Resour. Res., 52, doi: 10.1002/2015WR018236, 2016.

Andreasen, M., Andreasen, L. A., Jensen, K. H., Sonnenborg, T. O. and Bircher, S.: Estimation of Regional Groundwater Recharge Using Data from a Distributed Soil Moisture Network. Vadose Zone J, doi:10.2136/vzj2013.01.0035, 2013.

Baroni, G. and Oswald, S.E.: A scaling approach for the assessment of biomass changes and rainfall interception using cosmic-ray neutron sensing. Journal of Hydrology 525, 264–276. doi:10.1016/j.jhydrol.2015.03.053, 2015.

Baatz, R., Bogena, H. R., Hendricks Franssen, H.-J., Huisman, J. A., Montzka, C. and Vereecken, H.: An empirical vegetation correction for soil moisture content quantification using cosmic ray probes. Water Resour. Res., 51, doi: 10.1002/ 2014WR016443, 2015.

Bogena, H. R., J. A. Huisman, R. Baatz, H.-J. Hendricks Franssen, and H. Vereecken: Accuracy of the cosmic-ray soil water content probe in humid forest ecosystems: The worst case scenario. Water Resour. Res., 49, doi: 10.1002/wrcr.20463, 2013.

Boudreau, J., Nelson, R. F., Margolis, H. A., Beaudoin, A., Guindon, L., & Kimes, D. S.: Regional above ground forest biomass using airborne and spaceborne LiDAR in Québec. Remote sensing of environment, 112, 3876–3890, doi: 10.1016/j.rse.2008.06.003, 2008.

Chrisman, B. and M. Zreda: Quantifying mesoscale soil moisture with the cosmic-ray rover, Hydrology and Earth System Sciences Discussions 10, 7127-7160, doi: 10.5194/hessd-10-7127-2013, doi: 10.5194/hessd-10-7127-2013, 2013.

Desilets, D., Zreda, M. and Ferré, T. P. A.: Nature´s neutron probe: Land surface hydrology at an elusive scale with cosmic rays. Water Resour. Res., 46, W11505, doi:10.1029/2009WR008726, 2010.

Desilets, D., and Zreda, M.: Footprint diameter for a cosmic-ray soil moisture probe: Theory and Monte Carlo simulations. Water Resour. Res., 49, doi: 10.1002/wrcr.20187, 2013.

Dunkerley, D.: Measuring interception loss and canopy storage in dryland vegetation: a brief review and evaluation of available research strategies. Hydrological Processes, 14(4), pp.669-678, doi: 10.1002/(SICI)1099-1085(200003)14:43.0.CO;2-I, 2000.

Franz, T. E., Zreda, M., Rosolem, R. and Ferre, T.P.A.: Field Validation of a Cosmic-Ray Neutron Sensor Using a Distributed Sensor Network. Vadose Zone J., 2012, doi: 10.2136/vzj2012.0046, 2012.

Franz, T. E., Zreda, M. Rosolem, R., Hornbuckle, B. K., Irvin, S. L., Adams, H., Kolb, T. E., Zweck, C. and Shuttleworth, W. J.: Ecosystem-scale measurements of biomass water using cosmic ray neutrons. Geophys. Res. Lett., 40, 3929–3933, doi:10.1002/grl.50791, 2013a.

Franz, T. E., Zreda, M., Rosolem, R. and Ferré, T. P. A.: A universal calibration function for determination of soil moisture with cosmic-ray neutrons. Hydrol. Earth Syst. Sci., 17, 453–460, 2013b, doi: 10.5194/hess-17-453-2013, 2013b.

Franz, T. E., Wang, T., Avery, W., Finkenbiner, C. and Brocca, L.: Combined analysis of soil moisture measurements from roving and fixed cosmic ray neutron probes for multiscale real-time monitoring. Geophys. Res. Lett., 42, doi:10.1002/2015GL063963, 2015.

Glasstone, S. and Edlund, M. C.: The elements of nuclear reactor theory. 5th Edn., Van Nostrand, New York, 416 pp., 1952.

Hawdon, A., McJannet, D., and Wallace, J.: Calibration and correction procedures for cosmic-ray neutron soil moisture probes located across Australia, Water Resour. Res., 50, 5029–5043, doi:10.1002/2013WR015138, 2014.

Heidbüchel, I., Güntner, A. and Blume, T.: Use of cosmic-ray neutron sensors for soil moisture monitoring in forests. Hydrol. Earth Syst. Sci, 20, pp.1269-1288, doi:10.5194/hess-20-1269-2016, 2016.

Hornbuckle, B., Irvin, S., Franz, T., Rosolem, R. and Zweck, C.: The potential of the COSMOS network to be a source of new soil moisture information for SMOS and SMAP. In Geoscience and Remote Sensing Symposium (IGARSS), 2012 IEEE International, pp. 1243-1246, doi: 10.1109/IGARSS.2012.6351317, 2012.

Hughes, E. B. and Marsden, P. L.: Response of a standard IGY neutron monitor. Journal of Geophysical Research, 71(5), 1435-1444, doi: 10.1029/JZ071i005p01435, 1966.

Iwema, J., Rosolem, R., Baatz, R., Wagener, T., and Bogena, H. R.: Investigating temporal field sampling strategies for site-specific calibration of three soil moisture–neutron intensity parameterisation methods, Hydrol. Earth Syst. Sci., 19, 3203-3216, doi:10.5194/hess-19-3203-2015, 2015.

Jenkins, J. C., Chojnacky, D. C. Heath, L. S. and Birdsey, R. A.: National-Scale Biomass Estimators for United States Tree Species. Forest Science 49(1), 2003.

Knoll, G. F.: Radiation Detection and Measurement. Third Edition. John Wiley & Sons, Inc., 2010.

Köhli, M., Schrön, M., Zreda, M., Schmidt, U., Dietrich, P. and Zacharias, S.: Footprint characteristics revised for field-scale soil moisture monitoring with cosmic-ray neutrons. Water Resour. Res, 51(7), pp. 5772 – 5790, doi: 10.1002/2015WR017169, 2015.

Lal, R.: Carbon sequestration. Philosophical Transactions of the Royal Society of London B: Biological Sciences, 363(1492), pp. 815-830, doi:10.1098/rstb.2007.2185, 2008.

Levy, P.E., Hale, S.E. and Nicoll, B.C.: Biomass expansion factors and root : shoot ratios for coniferous tree species in Great Britain. Forestry, Vol. 77, No. 5, 2004, doi: 10.1093/forestry/77.5.421, 2004.

Nord-Larsen, T. and Schumacher, J.: Estimation of forest resources from a country wide laser scanning survey and national forest inventory data. Remote Sensing of Environment 119 (2012) 148–157, doi: 10.1016/j.rse.2011.12.022, 2012.

O'Kelly, B.: Accurate determination of moisture content of organic soils using the oven drying method, Drying Technology, 22(7), 1767-1776. doi: 10.1081/DRT-200025642, 2004.

Pelowitz, D. B.: MCNP6^{TM} User´s Manual, Version 1. Los Alamos National Laboratory report LA-CP-13-00634, Rev. 0, 2013.

Popescu, S.C.: Estimating biomass of individual pine trees using airborne lidar. Biomass and Bioenergy, 31(9), pp. 646-655, doi:10.1016/j.biombioe.2007.06.022, 2007.

Ringgaard, R., Herbst, M. and Friborg, T.: Partitioning forest evapotranspiration: Interception evaporation and the impact of canopy structure, local and regional advection. Journal of Hydrology 517 (2014) 677–690, doi: 10.1016/j.jhydrol.2014.06.007, 2014.

Rivera Villarreyes, C. A., Baroni, G. and Oswald, S. E.: Integral quantification of seasonal soil moisture changes in farmland by cosmic-ray neutrons. Hydrol. Earth Syst. Sci., 15, 3843–3859, doi:10.5194/hess-15-3843-2011, 2011.

Rosolem, R., Shuttleworth, W. J., Zreda, M., Franz, T. E., Zeng, X. and Kurc, S. A.: The Effect of Atmospheric Water Vapor on Neutron Count in the Cosmic-Ray Soil Moisture Observing System. Journal of hydrometeorology, doi: 10.1175/JHM-D-12-0120.1, 2013.

Salminen, R., Batista, M. J., Bidovec, M. etc.: Geochemical Atlas of Europe. Part 1: Background Information, Methodology and Maps. Espoo, Geological Survey of Finland, 526 pages, 36 figures, 362 maps, 2005.

Sears, V. F.: Neutron scattering lengths and cross sections. Neutron News, Vol. 3, No. 3, 1992, pp. 29-37, doi: 10.1080/10448639208218770, 1992.

Serup, H., Falster, H., Gamborg, C., Gundersen, P, etc.: Wood for Energy production. Technology - Environment – Economy Second Revised Edition, 2002.

Sigouin, M. J. P. and Si, B. C.: Calibration of a non-invasive cosmic-ray probe for wide area snow water equivalent measurement, The Cryosphere, 10, 1181-1190, doi:10.5194/tc-10-1181-2016, 2016.

Tian, Z., Li, Z., Liu, G., Li, B., and Ren, T.: Soil Water Content Determination with Cosmic-ray Neutron Sensor: Correcting Aboveground Hydrogen Effects with Thermal/Fast Neutron Ratio. Journal of Hydrology, doi:10.1016/j.jhydrol.2016.07.004, 2016.

Zreda, M., Desilets, D., Ferré, T. P. A. and Scott, R. L.: Measuring soil moisture content non-invasively at intermediate spatial scale using cosmic-ray neutrons. Geophysical Research Letters, Vol. 35, L21402, doi: 10.1029/2008GL035655, 2008.

Zreda, M., W. J. Shuttleworth, X. Zeng, C. Zweck, D. Desilets, T. Franz, and R. Rosolem: COSMOS: the cosmic-ray soil moisture observing system, Hydrol. Earth Syst. Sci., 16(11), 4079–4099, doi: 10.5194/hess-16-4079-2012, 2012.

Zweck, C., Zreda, M. and Desilets, D.: Snow shielding factors for cosmogenic nuclide dating inferred from Monte Carlo neutron transport simulations. Earth and Planetary Science Letters 379, 64–71, doi: 10.1016/j.epsl.2013.07.023, 2013.

Tables

Table 1 – Dynamics of different hydrogen pools.

	Static *Yearly*	Quasi-static *Sub-yearly*	Dynamic *Daily*
Soil moisture			x
Tree roots		x	
Soil organic matter		x	
Water in soil minerals	x		
Vegetation (cellulose, water)		x	x
Snow		x	x
Puddles			x
Open water (river, sea, lake)		x	
Canopy intercepted water			x
Buildings/roads	x		
Atmospheric water vapor			x

Table 2 – Average tree height, tree diameter and dry bulk density (bd_{dry}) of the litter layer and the mineral soil at Gludsted Plantation field site. Tree height and diameter are representative of conditions for year 2012.

	Average	Standard deviation	Max.	Min.
Tree height* [m]	11	6	25	3
Tree diameter* [m]	0.14	0.08	0.34	0.03
Dry bulk density litter layer, [g cm^{-3}]	0.34	0.29	1.09	0.09
Dry bulk density mineral soil, [g cm^{-3}]	1.09	0.28	1.53	0.22

* Data obtained from the Danish Nature Agency

Table 3 – Chemical composition of major elements at Gludsted Plantation determined using X-ray fluorescence analysis on soil samples collected in 0.20-0.25 m depth.

	Gludsted Plantation [%]
O	52.78
Si	44.86
Al	1.54
K	0.53
Ti	0.29

Table 4 – Forest properties used in modeling.

*Specific for model with forest conceptualization of Model *Tree trunk, Foliage, Air*. **Reference model.

	Models				
	No vegetation	50 t ha^{-1}	100 t ha^{-1}**	200 t ha^{-1}	400 t ha^{-1}
Dry above-ground biomass [t ha^{-1}]	0	50	100	200	400
Wet above-ground biomass [t ha^{-1}]	0	91	182	364	727
Dry below-ground biomass [t ha^{-1}]	0	12.5	25	50	100
Wet below-ground biomass [t ha^{-1}]	0	23	45	91	182
Tree trunk density [g cm^{-3}] *	-	0.83	0.83	0.83	0.83
Tree trunk radius [m] *	-	0.07	0.07	0.07	0.07
Tree height [m] *	-	25	25	25	25
Foliage density [g cm^{-3}] *	-	0.00134	0.00151	0.00185	0.00255
Foliage band [m] *	-	2.44	1.70	1.18	0.82
Sub-cell size [m x m] *	-	6.67 x 6.67	4.72 x 4.72	3.34 x 3.34	2.36 x 2.36

Table 5 – Modeled ground level (1.5 m) and canopy level (27.5 m) thermal neutron intensity and epithermal neutron intensity for the Gludsted Plantation models including four different forest canopy conceptualizations (see Fig. 3).

Models		Thermal 1.5 m	Thermal 27.5 m	Epithermal 1.5 m	Epithermal 27.5 m
~~Gludsted Plantation models (Fig. 3)~~	Foliage	573	207	681	813
-	Tree trunk, Air	484	272	610	695
-	Tree trunk, Foliage	536	261	619	716
	Tree trunk, Air, Foliage	504	257	623	717

Table 6 – Sensitivity in modeled ground level (1.5 m) and canopy level (27.5 m) thermal neutron intensity and epithermal neutron intensity due to (1) volumetric soil moisture, (2) soil chemistry, (3) litter layer thickness, (4) mineral soil and litter dry bulk density (bd_{dry}), (5) canopy interception and (6) biomass. The sensitivity is provided in absolute values and are relative to the simulations based on Model *Tree trunk, Air, Foliage** and Model *Foliage***, respectively (see Fig. 3 and Table 5). Values provided in parentheses specifies the direct effect of one-by-one excluding soil organic matter (*third order complexity*), Gd (*second order complexity*), below ground biomass (*first order complexity*) and site specific major elements soil chemistry (SiO_2).

Models		Thermal 1.5 m	Thermal 27.5 m	Epithermal 1.5 m	Epithermal 27.5 m
Soil moisture ~~models (Fig. 4)~~ (Fig. 4)	0.18 m^3 m^{-3}	504*	257*	623*	717*
	0.05 m^3 m^{-3}	100	47	131	109
-	0.10 m^3 m^{-3}	45	20	58	50
-	0.25 m^3 m^{-3}	-25	-12	-27	-23
-	0.35 m^3 m^{-3}	-47	-22	-53	-45
	0.45 m^3 m^{-3}	-59	-28	-69	-59
Soil moisture ~~models (Fig. 5)~~ (Fig. 5)	0.18 m^3 m^{-3}	573**	207**	681**	813**
	0.05 m^3 m^{-3}	119	40	142	115
-	0.10 m^3 m^{-3}	56	18	68	53
-	0.25 m^3 m^{-3}	-27	-9	-30	-23
-	0.35 m^3 m^{-3}	-50	-16	-55	-48
	0.45 m^3 m^{-3}	-64	-21	-74	-61

Formatted Table ... [1]
Formatted ... [2]
Deleted Cells ... [3]
Formatted ... [4]
Formatted ... [5]
Formatted ... [6]
Formatted ... [7]
Formatted Table ... [8]
Formatted ... [10]
Formatted ... [9]
Formatted ... [11]
Formatted ... [13]
Formatted ... [12]
Formatted ... [15]
Formatted ... [16]
Formatted ... [17]
Formatted ... [18]
Formatted ... [19]
Formatted ... [14]
Formatted ... [22]
Formatted ... [20]
Formatted ... [21]
Formatted ... [23]
Formatted ... [24]
Formatted ... [25]
Formatted ... [26]
Formatted ... [29]
Formatted ... [27]
Formatted ... [28]
Formatted ... [30]
Formatted ... [31]
Formatted ... [32]
Formatted ... [33]
Formatted ... [36]
Formatted ... [34]
Formatted ... [35]
Formatted ... [38]
Formatted ... [37]
Formatted ... [39]
Formatted ... [40]
Formatted ... [43]
Formatted ... [41]
Formatted ... [42]
Formatted ... [45]
Formatted ... [44]
Formatted ... [47]
Formatted ... [46]
Formatted ... [49]
Formatted ... [48]
Formatted ... [51]
Formatted ... [50]

Soil chemistry ~~models (Fig. 6)~~	4^{th} order complexity	504*	257*	623*	717*
	3^{rd} order complexity	19 (+19)	8 (+8)	25 (+25)	14 (+14)
	2^{nd} order complexity	18 (-1)	9 (+1)	27 (-2)	17 (+3)
	1^{st} order complexity	22 (+4)	10 (+1)	26 (-1)	18 (+1)
	SiO_2	27 (+5)	11 (+1)	23 (-3)	19 (+1)
Litter layer ~~models (Fig. 6A)~~	10.0 cm	504*	257*	623*	717*
(Fig. 6A)	7.5 cm	11	4	26	22
	5.0 cm	18	9	53	41
	2.5 cm	24	12	85	71
	No litter layer	22	17	131	113
Density ~~models~~	Gludsted Plantation*	504*	257*	623*	717*
	Higher litter layer bd_{dry}	-7	-5	-10	-6
	Higher mineral soil bd_{dry}	15	5	17	10
	Lower litter layer bd_{dry}	7	2	14	10
	Lower mineral soil bd_{dry}	-26	-13	-22	-18
Canopy interception ~~models (Fig. 6B)~~	Dry canopy	504*	257*	623*	717*
(Fig. 6B)	1 mm	4	-2	-3	0
	2 mm	7	-3	-5	5
	4 mm	15	-7	-5	2
Biomass ~~models (Fig. 6C)~~	100 t ha^{-1}	504*	257*	623*	717*
(Fig. 6C)	No vegetation	-67	-21	99	85
	50 t ha^{-1}	-16	-8	45	33
	200 t ha^{-1}	14	2	-70	-47
	400 t ha^{-1}	21	2	-172	-116
Biomass ~~models (Fig. 6D)~~	100 t ha^{-1}	573**	207**	681**	813**
(Fig. 6D)	No vegetation	-136	29	41	-28
	50 t ha^{-1}	0	24	13	-23
	200 t ha^{-1}	-9	-32	-26	22
	400 t ha^{-1}	-48	-59	-82	73

Formatted ... [52]
Formatted ... [53]
Formatted ... [54]
Formatted ... [55]
Formatted ... [56]
Formatted ... [57]
Formatted ... [60]
Formatted ... [61]
Formatted ... [62]
Formatted ... [63]
Formatted ... [64]
Formatted ... [59]
Formatted ... [58]
Formatted ... [65]
Formatted ... [66]
Formatted ... [67]
Formatted ... [68]
Formatted ... [69]
Formatted ... [70]
Formatted ... [71]
Formatted ... [72]
Formatted ... [73]
Formatted ... [74]
Formatted ... [75]
Formatted ... [76]
Formatted ... [77]
Formatted ... [78]
Formatted ... [79]
Formatted ... [80]
Formatted ... [81]
Formatted ... [82]
Formatted ... [83]
Formatted ... [84]
Formatted ... [85]
Formatted ... [86]
Formatted ... [87]
Formatted ... [88]
Formatted ... [89]
Formatted ... [90]
Formatted ... [91]
Formatted ... [92]
Formatted ... [93]
Formatted ... [94]
Formatted ... [95]
Formatted ... [96]
Formatted ... [97]
Formatted ... [98]
Formatted ... [99]
Formatted ... [100]
Formatted ... [101]
Formatted ... [102]
Formatted ... [103]
Formatted ... [104]
Formatted ... [105]
Formatted ... [106]
Formatted ... [107]
Formatted ... [108]
Formatted ... [109]
Formatted ... [110]
Formatted ... [111]
Formatted ... [112]

Figures

Figure 1 – Map showing the location of the three field sites; G: Gludsted Plantation (green), V: Voulund Farmland (beige) and H: Harrild Heathland (purple). The circles represent the footprint of the neutron detector (radius = 300 m).

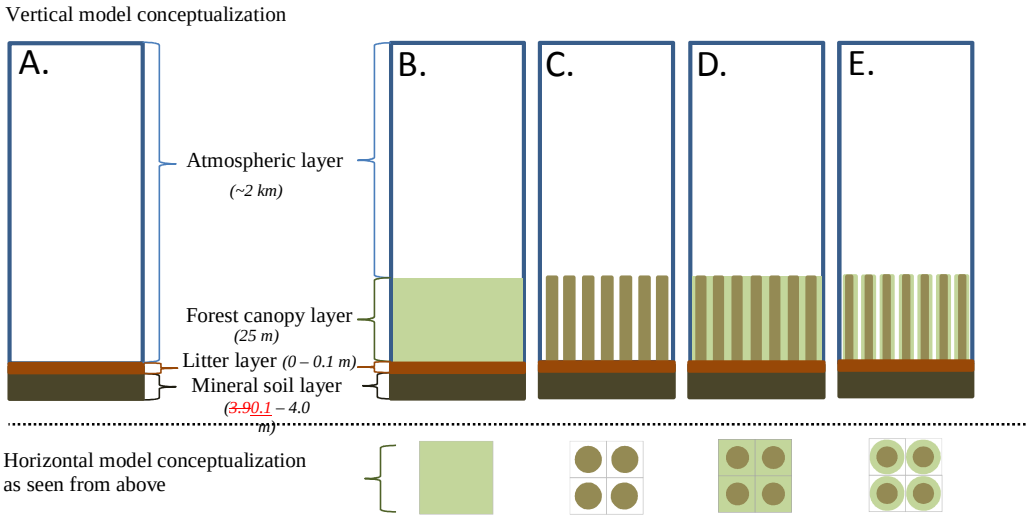

Figure 2 – Model conceptualizations of forest. (A) no forest canopy layer (model name: *0 t ha^{-1}*); (B) homogeneous foliage layer with a uniformly distributed biomass (model name: *Foliage*); (C) cylindrical tree trunks with air in between (model name: *Tree trunks, Air*); (D) cylindrical tree trunks with foliage in between (model name: *Tree Trunks, Foliage*); (E) cylindrical tree trunks enveloped in a foliage-cover with air in between (model name: *Tree trunks, Foliage, Air*). The bottom four figures illustrate the forest conceptualization seen from above.

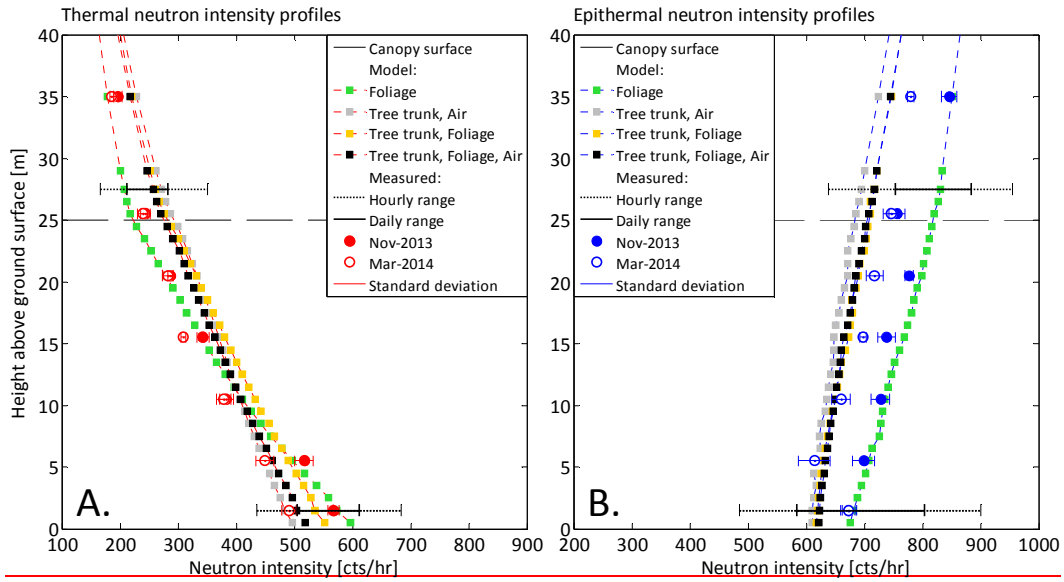
Thermal neutron intensity profiles
Epithermal neutron intensity profiles
Height above ground surface [m]
Neutron intensity [cts/hr]
Canopy surface
Model:
Foliage
Tree trunk, Air
Tree trunk, Foliage
Tree trunk, Foliage, Air
Measured:
Hourly range
Daily range
Nov-2013
Mar-2014
Standard deviation
A.
B.

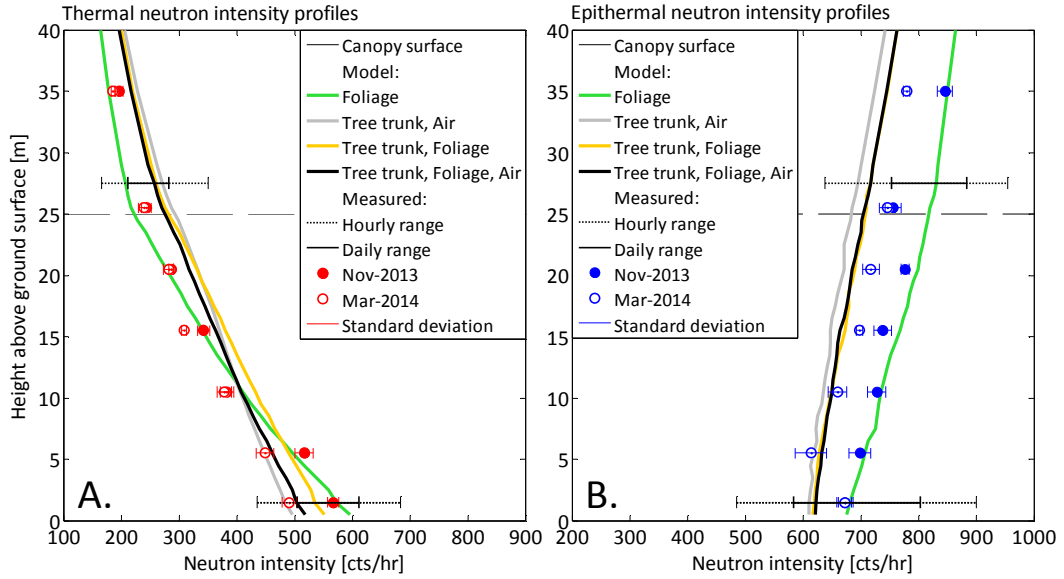
Thermal neutron intensity profiles
Epithermal neutron intensity profiles
Height above ground surface [m]
Neutron intensity [cts/hr]
Canopy surface
Model:
Foliage
Tree trunk, Air
Tree trunk, Foliage
Tree trunk, Foliage, Air
Measured:
Hourly range
Daily range
Nov-2013
Mar-2014
Standard deviation
A.
B.

Figure 3 – Measured and modeled (A) thermal and (B) epithermal neutron intensity profiles at Gludsted Plantation. Hourly and daily ranges of variation of thermal and epithermal neutron intensities at ground and canopy level for the period 2013–2015. Gludsted Plantation is modeled using four different forest canopy conceptualizations (see Figure 2).

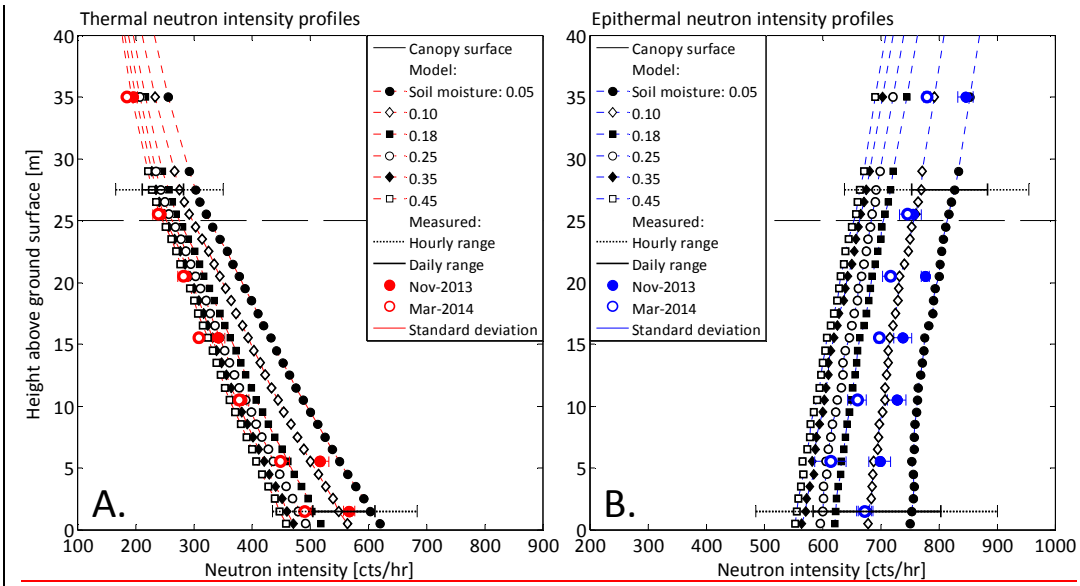

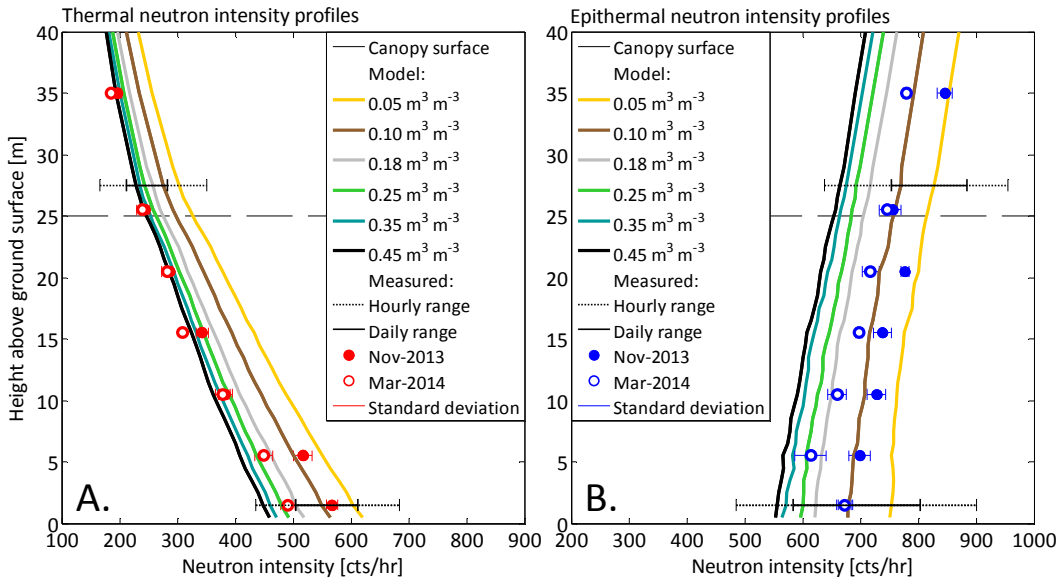

Figure 4 – Sensitivity to volumetric soil moisture~~, in m^3 m^{-3} (~~ using Model *Tree trunk, Foliage, Air*~~).~~. Measured and modeled (A) thermal and (B) epithermal neutron intensity profiles at Gludsted Plantation. Hourly and daily ranges of variation of thermal and epithermal neutron intensities at ground and canopy level for the period 2013–2015.

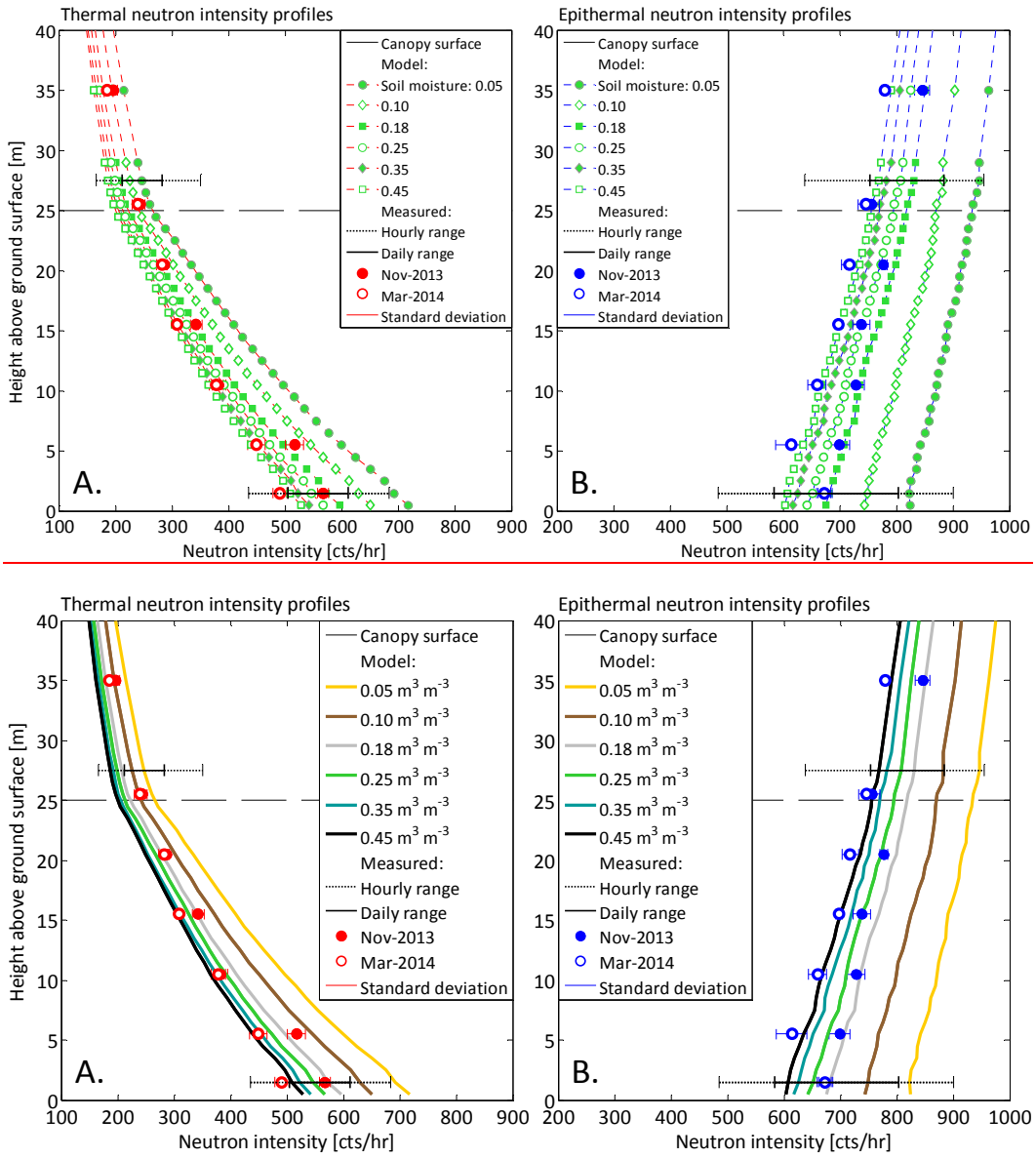

Figure 5 - Sensitivity to volumetric soil moisture~~, in m^3 m^{-3} (~~ using Model *Foliage*~~).~~. Measured and modeled (A) thermal and (B) epithermal neutron intensity profiles at Gludsted Plantation. Hourly and daily ranges of variation of thermal and epithermal neutron intensities at ground and canopy level for the period 2013–2015.

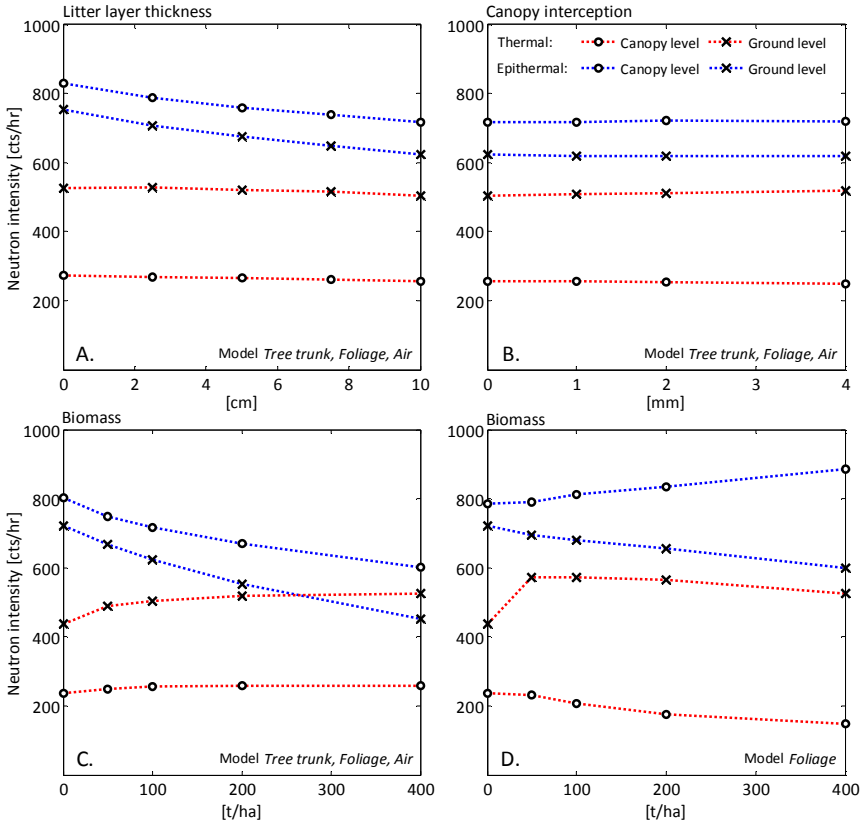

Figure 6 – Sensitivity of ground and canopy level thermal and epithermal neutron intensity to (A) litter layer thickness using Model *Tree trunk*, *Foliage*, *Air*, (B) canopy interception using Model *Tree trunk*, *Foliage*, *Air*, biomass using (C) Model *Tree trunk*, *Foliage*, *Air* and (D) Model *Foliage*, respectively.

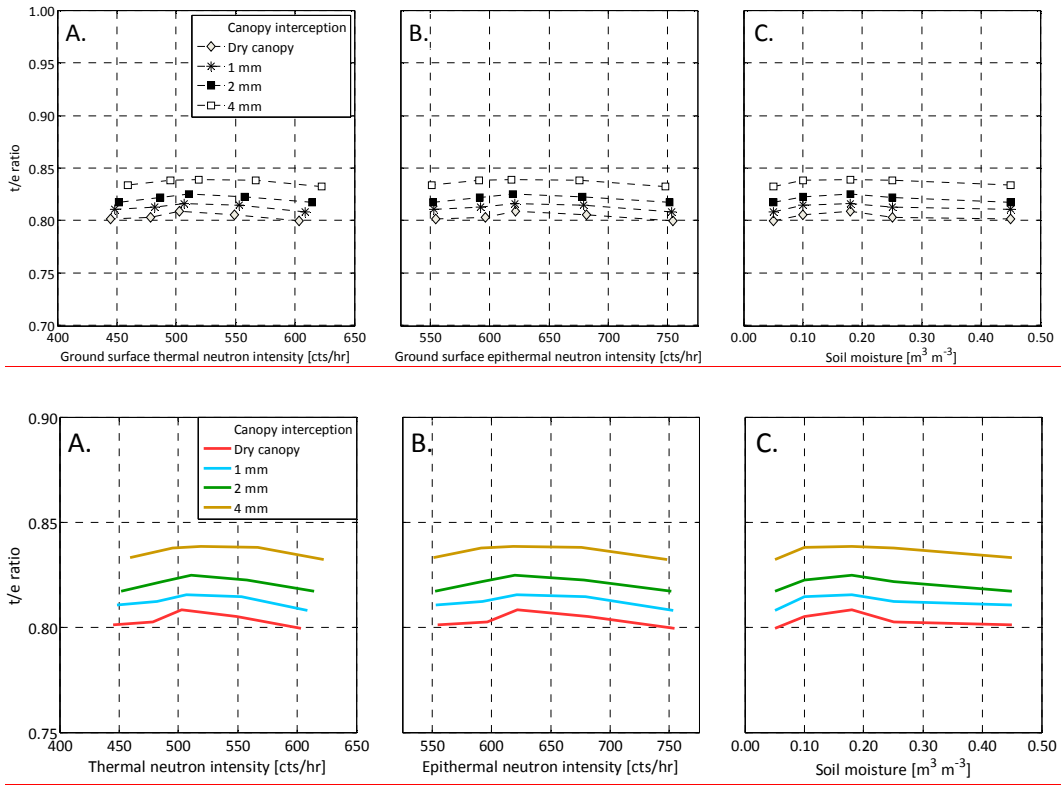

Figure 7 – Modeled ground level thermal-to-epithermal neutron intensity ratios using the Model *Tree trunk, Foliage, Air* for a dry forest canopy and canopy interception of 1 mm, 2 mm and 4 mm. plotted against modeled: (A) ground level thermal neutron intensity, (B) ground level epithermal neutron intensity, and (C) volumetric soil moisture.

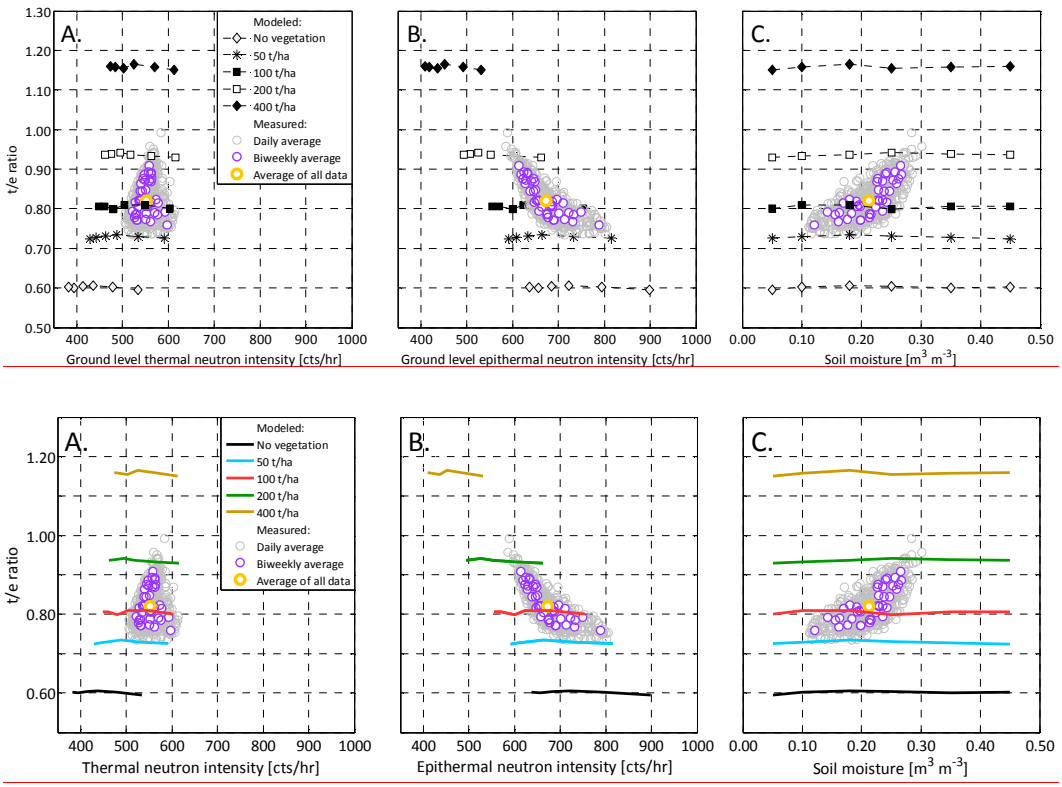

Figure 8 – Neutron intensities measured at Gludsted Plantation in the time period 2013-2015 and modeled using the Model *Tree trunk, Foliage, Air*. Ground level thermal-to-epithermal neutron intensity ratio plotted against measured and modeled: (A) ground level thermal neutron intensity, (B) ground level epithermal neutron intensity, and (C) volumetric soil moisture.

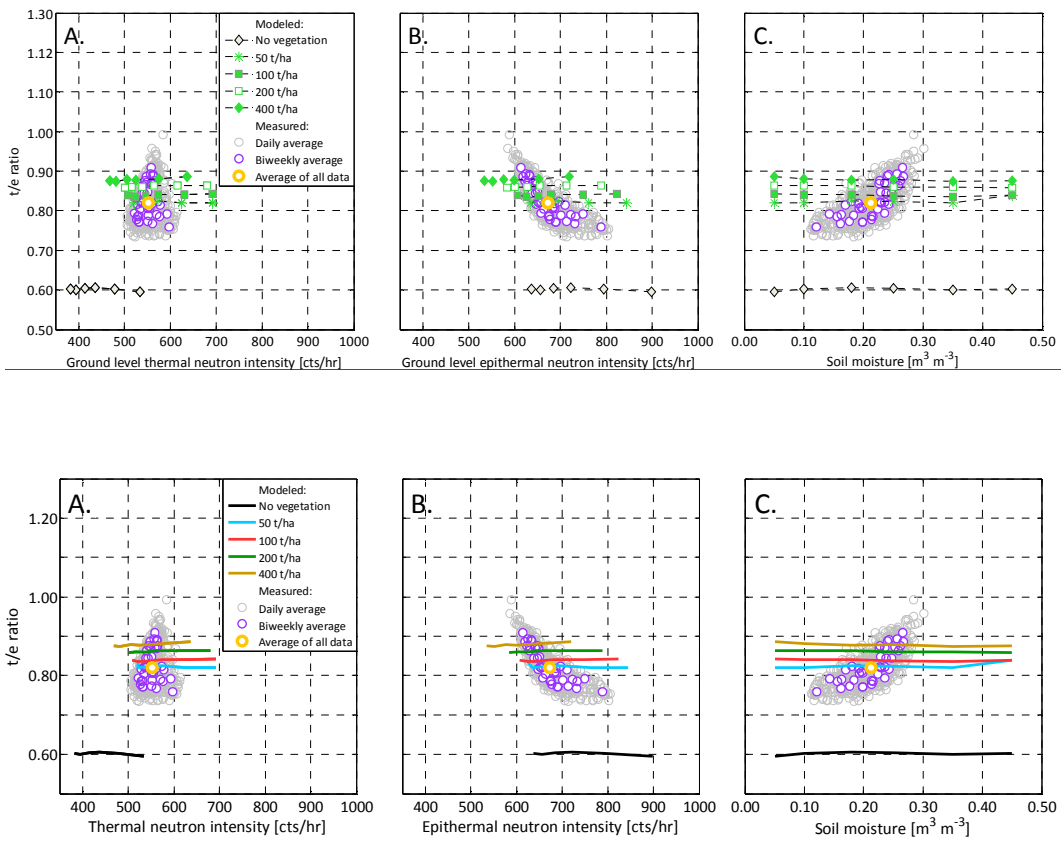

Figure 9 – Neutron intensities measured at Gludsted Plantation in the time period 2013-2015 and modeled using the Model *Foliage*. Ground level thermal-to-epithermal neutron intensity ratio plotted against measured and modeled: (A) ground level thermal neutron intensity, (B) ground level epithermal neutron intensity, and (C) volumetric soil moisture.

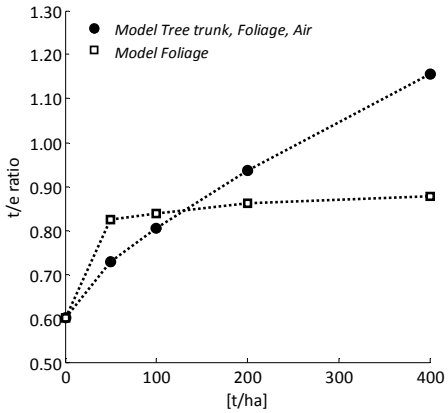

Figure 10 – Ground level thermal-to-epithermal neutron ratio plotted against biomass equivalent to dry above-ground biomass of: 50 t/ha, 100 t/ha (Gludsted Plantation), 200 t/ha and 400 t/ha using Model *Tree trunk, Foliage, Air* and Model *Foliage*, respectively.

Page 28: [1] Formatted Table **Mie Andreasen** **3/7/2017 2:13:00 PM**

Formatted Table

Page 28: [2] Formatted **Mie Andreasen** **3/7/2017 2:13:00 PM**

Line spacing: single

Page 28: [3] Deleted Cells **Mie Andreasen** **3/7/2017 2:13:00 PM**

Deleted Cells

Page 28: [4] Formatted **Mie Andreasen** **3/7/2017 2:13:00 PM**

Line spacing: single

Page 28: [5] Formatted **Mie Andreasen** **3/7/2017 2:13:00 PM**

Line spacing: single

Page 28: [6] Formatted **Mie Andreasen** **3/7/2017 2:13:00 PM**

Line spacing: single

Page 28: [7] Formatted **Mie Andreasen** **3/7/2017 2:13:00 PM**

Line spacing: single

Page 28: [8] Formatted Table **Mie Andreasen** **3/7/2017 2:13:00 PM**

Formatted Table

Page 28: [9] Formatted **Mie Andreasen** **3/7/2017 2:13:00 PM**

Centered, Line spacing: single

Page 28: [10] Formatted **Mie Andreasen** **3/7/2017 2:13:00 PM**

Line spacing: single

Page 28: [11] Formatted **Mie Andreasen** **3/7/2017 2:13:00 PM**

Line spacing: single

Page 28: [12] Formatted **Mie Andreasen** **3/7/2017 2:13:00 PM**

English (U.S.)

Page 28: [12] Formatted **Mie Andreasen** **3/7/2017 2:13:00 PM**

English (U.S.)

Page 28: [13] Formatted **Mie Andreasen** **3/7/2017 2:13:00 PM**

Font color: Black, Danish

Page 28: [13] Formatted **Mie Andreasen** **3/7/2017 2:13:00 PM**

Font color: Black, Danish

Page 28: [14] Formatted **Mie Andreasen** **3/7/2017 2:13:00 PM**

Line spacing: single

Page 28: [15] Formatted **Mie Andreasen** **3/7/2017 2:13:00 PM**

Font color: Black, Danish

Page 28: [15] Formatted **Mie Andreasen** **3/7/2017 2:13:00 PM**

Font color: Black, Danish

Page 28: [16] Formatted **Mie Andreasen** **3/7/2017 2:13:00 PM**

English (U.S.)

Page 28: [17] Formatted **Mie Andreasen** **3/7/2017 2:13:00 PM**

English (U.S.)

Page 28: [18] Formatted **Mie Andreasen** **3/7/2017 2:13:00 PM**

English (U.S.)

Page 28: [19] Formatted **Mie Andreasen** **3/7/2017 2:13:00 PM**

English (U.S.)

Page 28: [20] Formatted **Mie Andreasen** **3/7/2017 2:13:00 PM**

Line spacing: single

Page 28: [21] Formatted **Mie Andreasen** **3/7/2017 2:13:00 PM**

English (U.S.)

Page 28: [22] Formatted **Mie Andreasen** **3/7/2017 2:13:00 PM**

Font color: Black, Danish

Page 28: [22] Formatted **Mie Andreasen** **3/7/2017 2:13:00 PM**

Font color: Black, Danish

Page 28: [23] Formatted **Mie Andreasen** **3/7/2017 2:13:00 PM**

English (U.S.)

Page 28: [24] Formatted **Mie Andreasen** **3/7/2017 2:13:00 PM**

English (U.S.)

Page 28: [25] Formatted **Mie Andreasen** **3/7/2017 2:13:00 PM**

English (U.S.)

Page 28: [26] Formatted **Mie Andreasen** **3/7/2017 2:13:00 PM**

English (U.S.)

Page 28: [27] Formatted **Mie Andreasen** **3/7/2017 2:13:00 PM**

Line spacing: single

Page 28: [28] Formatted **Mie Andreasen** **3/7/2017 2:13:00 PM**

English (U.S.)

Page 28: [29] Formatted **Mie Andreasen** **3/7/2017 2:13:00 PM**

Font color: Black

Page 28: [29] Formatted **Mie Andreasen** **3/7/2017 2:13:00 PM**

Font color: Black

Page 28: [30] Formatted **Mie Andreasen** **3/7/2017 2:13:00 PM**

English (U.S.)

Page 28: [31] Formatted **Mie Andreasen** **3/7/2017 2:13:00 PM**

English (U.S.)

Page 28: [32] Formatted **Mie Andreasen** **3/7/2017 2:13:00 PM**

English (U.S.)

Page 28: [33] Formatted **Mie Andreasen** **3/7/2017 2:13:00 PM**

English (U.S.)

Page 28: [34] Formatted **Mie Andreasen** **3/7/2017 2:13:00 PM**

Line spacing: single

Page 28: [35] Formatted **Mie Andreasen** **3/7/2017 2:13:00 PM**

English (U.S.)

Page 28: [36] Formatted **Mie Andreasen** **3/7/2017 2:13:00 PM**

Font color: Black

Page 28: [37] Formatted **Mie Andreasen** **3/7/2017 2:13:00 PM**

Line spacing: single

Page 28: [38] Formatted **Mie Andreasen** **3/7/2017 2:13:00 PM**

Font color: Black

Page 28: [39] Formatted **Mie Andreasen** **3/7/2017 2:13:00 PM**

Line spacing: single

Page 28: [40] Formatted **Mie Andreasen** **3/7/2017 2:13:00 PM**

Font color: Black

Page 28: [41] Formatted **Mie Andreasen** **3/7/2017 2:13:00 PM**

English (U.S.)

Page 28: [42] Formatted **Mie Andreasen** **3/7/2017 2:13:00 PM**

Line spacing: single

Page 28: [43] Formatted **Mie Andreasen** **3/7/2017 2:13:00 PM**

Font color: Black

Page 28: [44] Formatted **Mie Andreasen** **3/7/2017 2:13:00 PM**

Line spacing: single

Page 28: [45] Formatted **Mie Andreasen** **3/7/2017 2:13:00 PM**

Font color: Black

Page 28: [46] Formatted **Mie Andreasen** **3/7/2017 2:13:00 PM**

Line spacing: single

Page 28: [47] Formatted **Mie Andreasen** **3/7/2017 2:13:00 PM**

Font color: Black

Page 28: [48] Formatted **Mie Andreasen** **3/7/2017 2:13:00 PM**

Line spacing: single

Page 28: [49] Formatted **Mie Andreasen** **3/7/2017 2:13:00 PM**

Font color: Black

Page 28: [50] Formatted **Mie Andreasen** **3/7/2017 2:13:00 PM**

Line spacing: single

Page 28: [51] Formatted **Mie Andreasen** **3/7/2017 2:13:00 PM**

Font color: Black

Page 29: [52] Formatted **Mie Andreasen** **3/7/2017 2:13:00 PM**

Line spacing: single

Page 29: [53] Formatted **Mie Andreasen** **3/7/2017 2:13:00 PM**

Line spacing: single

Page 29: [54] Formatted **Mie Andreasen** **3/7/2017 2:13:00 PM**

Line spacing: single

Page 29: [55] Formatted **Mie Andreasen** **3/7/2017 2:13:00 PM**

Line spacing: single

Page 29: [56] Formatted **Mie Andreasen** **3/7/2017 2:13:00 PM**

Line spacing: single

Page 29: [57] Formatted **Mie Andreasen** **3/7/2017 2:13:00 PM**

Line spacing: single

Page 29: [58] Formatted **Mie Andreasen** **3/7/2017 2:13:00 PM**

Line spacing: single

Page 29: [59] Formatted **Mie Andreasen** **3/7/2017 2:13:00 PM**

Font: Calibri, 11 pt

Page 29: [60] Formatted **Mie Andreasen** **3/7/2017 2:13:00 PM**

English (U.S.)

Page 29: [61] Formatted **Mie Andreasen** **3/7/2017 2:13:00 PM**

English (U.S.)

Page 29: [62] Formatted **Mie Andreasen** **3/7/2017 2:13:00 PM**

English (U.S.)

Page 29: [63] Formatted **Mie Andreasen** **3/7/2017 2:13:00 PM**

English (U.S.)

Page 29: [64] Formatted **Mie Andreasen** **3/7/2017 2:13:00 PM**

English (U.S.)

Page 29: [65] Formatted **Mie Andreasen** **3/7/2017 2:13:00 PM**

Line spacing: single

Page 29: [66] Formatted **Mie Andreasen** **3/7/2017 2:13:00 PM**

English (U.S.)

Page 29: [67] Formatted **Mie Andreasen** **3/7/2017 2:13:00 PM**

English (U.S.)

Page 29: [68] Formatted **Mie Andreasen** **3/7/2017 2:13:00 PM**

English (U.S.)

Page 29: [69] Formatted **Mie Andreasen** **3/7/2017 2:13:00 PM**

English (U.S.)

Page 29: [70] Formatted **Mie Andreasen** **3/7/2017 2:13:00 PM**

English (U.S.)

Page 29: [71] Formatted **Mie Andreasen** **3/7/2017 2:13:00 PM**

English (U.S.)

Page 29: [72] Formatted **Mie Andreasen** **3/7/2017 2:13:00 PM**

Line spacing: single

Page 29: [73] Formatted **Mie Andreasen** **3/7/2017 2:13:00 PM**

English (U.S.)

Page 29: [74] Formatted **Mie Andreasen** **3/7/2017 2:13:00 PM**

English (U.S.)

Page 29: [75] Formatted **Mie Andreasen** **3/7/2017 2:13:00 PM**

English (U.S.)

Page 29: [76] Formatted **Mie Andreasen** **3/7/2017 2:13:00 PM**

English (U.S.)

Page 29: [77] Formatted **Mie Andreasen** **3/7/2017 2:13:00 PM**

English (U.S.)

Page 29: [78] Formatted **Mie Andreasen** **3/7/2017 2:13:00 PM**

Danish

Page 29: [78] Formatted **Mie Andreasen** **3/7/2017 2:13:00 PM**

Danish

Page 29: [79] Formatted **Mie Andreasen** **3/7/2017 2:13:00 PM**

Line spacing: single

Page 29: [80] Formatted **Mie Andreasen** **3/7/2017 2:13:00 PM**

English (U.S.)

Page 29: [81] Formatted **Mie Andreasen** **3/7/2017 2:13:00 PM**

English (U.S.)

Page 29: [82] Formatted **Mie Andreasen** **3/7/2017 2:13:00 PM**

English (U.S.)

Page 29: [83] Formatted **Mie Andreasen** **3/7/2017 2:13:00 PM**

English (U.S.)

Page 29: [84] Formatted **Mie Andreasen** **3/7/2017 2:13:00 PM**

English (U.S.)

Page 29: [85] Formatted **Mie Andreasen** **3/7/2017 2:13:00 PM**

Line spacing: single

Page 29: [86] Formatted **Mie Andreasen** **3/7/2017 2:13:00 PM**

Font: Calibri, 11 pt

Page 29: [87] Formatted **Mie Andreasen** **3/7/2017 2:13:00 PM**

Line spacing: single

Page 29: [88] Formatted **Mie Andreasen** **3/7/2017 2:13:00 PM**

Line spacing: single

Page 29: [89] Formatted **Mie Andreasen** **3/7/2017 2:13:00 PM**

Line spacing: single

Page 29: [90] Formatted **Mie Andreasen** **3/7/2017 2:13:00 PM**

Line spacing: single

Page 29: [91] Formatted **Mie Andreasen** **3/7/2017 2:13:00 PM**

Line spacing: single

Page 29: [92] Formatted **Mie Andreasen** **3/7/2017 2:13:00 PM**

Line spacing: single

Page 29: [93] Formatted **Mie Andreasen** **3/7/2017 2:13:00 PM**

Line spacing: single

Page 29: [94] Formatted **Mie Andreasen** **3/7/2017 2:13:00 PM**

Line spacing: single

Page 29: [95] Formatted **Mie Andreasen** **3/7/2017 2:13:00 PM**

Line spacing: single

Page 29: [96] Formatted **Mie Andreasen** **3/7/2017 2:13:00 PM**

Font color: Black

Page 29: [97] Formatted **Mie Andreasen** **3/7/2017 2:13:00 PM**

Line spacing: single

Page 29: [98] Formatted **Mie Andreasen** **3/7/2017 2:13:00 PM**

Font: Calibri, 11 pt

Page 29: [99] Formatted **Mie Andreasen** **3/7/2017 2:13:00 PM**

Line spacing: single

Page 29: [100] Formatted **Mie Andreasen** **3/7/2017 2:13:00 PM**

Font color: Black

Page 29: [101] Formatted **Mie Andreasen** **3/7/2017 2:13:00 PM**

Line spacing: single

Page 29: [102] Formatted **Mie Andreasen** **3/7/2017 2:13:00 PM**

Font color: Black

Page 29: [103] Formatted **Mie Andreasen** **3/7/2017 2:13:00 PM**

Line spacing: single

Page 29: [104] Formatted **Mie Andreasen** **3/7/2017 2:13:00 PM**

Font color: Black

Page 29: [105] Formatted **Mie Andreasen** **3/7/2017 2:13:00 PM**

Line spacing: single

Page 29: [106] Formatted **Mie Andreasen** **3/7/2017 2:13:00 PM**

Font color: Black

Page 29: [107] Formatted **Mie Andreasen** **3/7/2017 2:13:00 PM**

Line spacing: single

Page 29: [108] Formatted **Mie Andreasen** **3/7/2017 2:13:00 PM**

Line spacing: single

Page 29: [109] Formatted **Mie Andreasen** **3/7/2017 2:13:00 PM**

Font color: Black

Page 29: [110] Formatted **Mie Andreasen** **3/7/2017 2:13:00 PM**

Line spacing: single

Page 29: [111] Formatted **Mie Andreasen** **3/7/2017 2:13:00 PM**

Font color: Black

Page 29: [112] Formatted **Mie Andreasen** **3/7/2017 2:13:00 PM**

Line spacing: single

Page 29: [113] Formatted **Mie Andreasen** **3/7/2017 2:13:00 PM**

Font color: Black